3-20-2019 1:00 PM

Neural correlates of enhanced attentional filtering of distractors across vs. within visual hemifields in the lateral prefrontal cortex

Maryam Nouri Kadijani, *The University of Western Ontario*

Supervisor: Martinez T.J., *The University of Western Ontario*
Co-Supervisor: Diedrichsen J., *The University of Western Ontario*
A thesis submitted in partial fulfillment of the requirements for the Master of Science degree in Neuroscience

ABSTRACT

Attention allows us to focus on only important sensory stimuli in a world full of distractors. However, the ability to allocate attention to important targets becomes more difficult when the distractors are located within the same visual hemifield as compared to when they are in the opposite visual hemifield. The neural mechanisms underlying this effect remains unclear. We recorded neuronal responses in lateral prefrontal cortex (LPFC), an area involved in the generation of signals related to attention, of two macaque monkeys while they performed a covert spatial attention task in two different conditions. Two stimuli were either separate in the left and right visual hemifield or both within the same visual hemifield. Consistent with previous studies, behavioral performance was lower in the within than in the across condition. Moreover, the proportion of single neurons in the LPFC showing selectivity for the attended location was significantly reduced in the within relative to the across condition. Additionally, we demonstrate that the activity of single neurons and simultaneous neuronal ensembles in the primate LPFC, can accurately decode attentional signals in the across condition rather than in the within condition. Ensemble decoding accuracy was sensitive to the noise correlation structure and dynamics of the neural ensembles. Our findings provide a neurophysiological correlate of the behavioral anisotropy observed during tasks that required attending to targets and distractors in different vs same hemifields. They further suggest that anisotropies in the representation of space by individual neurons and neuronal ensembles in the LPFC determine the efficiency of attentional filtering performance in primates.

Key Words: Lateral prefrontal cortex (LPFC), Allocation of Attention, Macaque, Across hemifields, Within hemifield, Multi electrode array (MEA), Neural ensemble.

Co-Authorship Statement

This thesis will comprise work as a journal article. The contributors to this paper are Maryam Nouri Kadijani, Theda Backen, Stefan Treue, Julio C. Martinez-Trujillo, Jörn Diedrichsen. M. Nouri K. analyzed the data and wrote the paper; T. Backen collected the data and wrote paper; S. Treue and J. Martinez devised the experiment and J. Diedrichsen supervised data analysis.

ACKNOWLEDGEMENTS

First of all, I would like to express my sincere gratitude to my supervisor, Dr. Julio Martinez-Trujillo. I am forever grateful for the chance he took on me as an inexperienced student. At many stages in the course of this research project, I greatly benefited from his scientific and non-scientific advices, particularly when I was feeling disappointed. I have been extremely lucky to have a supervisor who cared so much about my life both as a mother and as a student.

Besides my supervisor, I would also like to thank my co-supervisor Dr. Jorn Diedrichsen and my advisory committee, Dr. Stefan Everling and Dr. Brian Corneil, for their insightful comments and encouragements, but also for their challenging questions which incented me to widen my research from various perspectives.

Completing this work would have been much more difficult without the support and friendship provided by my labmates. I owe them so many insights, so many memories, and so many joyful moments. I have been incredibly fortunate to evolve surrounded by such exceptional lab family throughout my studies.

My sincere thanks also go to Benjamin Corrigan, Megan Roussy and Maryam Ghahremani for their valuable comments on this manuscript. Without they precious support it would not have been possible to write this thesis.

I am truly grateful to my parents for their immeasurable love and care. They have always encouraged me to explore my potentials and pursue my dreams to be where I am today in my life. I would like to thank my husband and my love (Hossein) for supporting me and keeping me motivated throughout this journey. I love you forever.

Finally, sweet thanks also go to my little son (Daniel) for making my life worth living.

TABLE OF CONTENTS

LIST OF TABLES

LIST OF FIGURES

Chapter 1

Introduction

At any given moment, we are exposed to much more sensory information from our environment than our brain is able to process simultaneously. Therefore, only a subset of sensory information can be process by human brain at any given moment. Why are we so cognitively limited? We can answer this question by knowing limitations of information processing in our brain.

First of all, our brain has a limited bandwidth of communication system, which is approximately one terabit information per second (Laughlin, Sejnowski, 2003). Secondly, information processing is energetically costly; it takes approximately 104 ATP molecules to transfer one bit of information through a chemical synapse (Steveninck, Laughlin, 1996). Considering this, the full bandwidth of the brain communication system for a day would entail an energy consumption of $\sim 7,400$ kcal. This amounts to 15 times more than what human brain (i.e. a brain with a size of 1300 to 1400 grams or approximately 3 pounds) actually consumes over the course of a day (i.e. ~ 500 kcal). Accordingly, only a subset of neurons (i.e. basic units of brain) can be active at any given moment (Levy, Baxter, 1996). Additionally, higher neural activation is disproportionally costly for a biological system, especially when maintained over extended periods of time (Laughlin, Sejnowski, 2003).

Therefore, for biological and economical reasons, the brain has a limited capacity to cognitively process the information that it receives from sensory systems about its environment. A selection process is thus required to select the relevant attributes of sensory information for prioritized processing. A decision by which sources of information are selected for further cognitive processing is known as selective attention (Yuntis, 2008; James, 1890).

1.1 Selective Attention

Attention is the cognitive process of selectivity concentrating on one aspect of the external or internal environment while ignoring other aspects. Intelligent behavior requires selecting task-relevant information and minimizing interference from irrelevant information. Hence, selective attention can refer to the processes that allow an individual to select and focus on a specific input for further processing while simultaneously suppressing distractor information. Since most studies in the literature have focused on filtering of the visual information, this work will focus on the visual selective attention.

Visual selective attention can be divided into two general categories: one is voluntary attention, also referred to as 'top-down' or 'endogenous attention' , like the attention given to this text you are currently reading. Second is the automatic or stimulus driven attention, which is referred to as 'bottom-up' or 'exogenous attention', such as a fast-moving object in our visual field. The most distinguishing factor between the two is the difference in their time courses. Endogenous attention requires a few hundred milliseconds to fully develop and can be maintained with effort. Whereas, exogenous attention happens within 100 to 120 milliseconds and diminishes rapidly (MacLean, 2009).

Visual selective attention can further be categorized based on the source of information that drives attention. 'Visual spatial attention' involves the allocation of attention toward certain coordinate in our visual field. Spatial attention can be concentrated on a very small area of visual field or be spread across a wider area (Laberge, Brown, 1986). In the latter case, the wider the spread, the less efficient is the processing of information (Castiello, Umiltà, 1990).

Attention can be allocated to specific features, such as color or motion direction. 'Feature-based attention' improves the representation of object characteristics throughout the visual field. It is a useful mechanism when searching for a specific stimulus feature such as looking for someone with a blue shirt in a crowd of people, or expecting a movement among a set of stable objects. In these cases, you are enhancing your ability to detect that specific

feature regardless of its location in space.

Lastly, attention can be deployed towards specific objects of interest. This 'object-based attention' is the one you use when trying to find a specific object in your environment (e.g. your keys). In this case, the combination of all the features and not just a single attribute of the target object, becomes highly salient, so that the object can be identified quickly among a set of other similar objects (Carrasco, 2011).

In all described forms of attention, feature-based, object-based, or spatial location, attention is processed at the expense of other visual informaion. This selection process requires that some of the visual information that enters our sensory system via the retina be disregarded at a downstream level, making us 'perceptively blind' to those stimuli. One question that may be asked is: what is the neural mechanism underlying this selection process? Using in vivo electrophysiological recording developed in the 1950's (Hubel, 1957; Green, 1958), neuroscientists have pursued to provide answer to this question.

1.2 Electrophysiology of Selective Attention

Neuronal electrophysiological recording is the study of the electrical properties of neurons, usually voltage or current, in particular action potential activity. Changes in these properties enable the nervous system to execute its functions, which are not only responsible for keeping us alive but also allow us to attain higher levels of cognition.

Electrophysiology of attention illuminates the fundamental mechanisms of attention in the temporal dynamics of neural response (Desimone, Duncan, 1995; Buschman, Kastner, 2015). One fundamental observation was obtained from single cell recording from visual cortex, prestriate area V4, of two rhesus monkeys trained to attend to stimuli at one location in the visual field and ignore other stimuli in different or same location. When both locations were within the receptive field of a cell, the response to the unattended stimulus was significantly decreased (Figure 1.1). The results showed that the enhancement of relevant signal and suppression of others might highlight the neural competition to identify

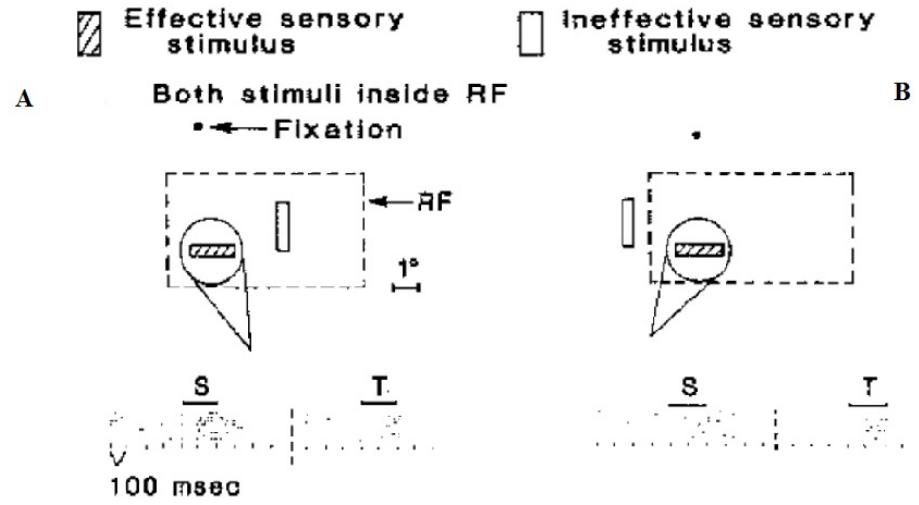

Figure 1.1: **Effect of Selective Attention on the Responses of a Neuron**

(A) Responses when monkey attended to one location inside the receptive field (RF) (S) and ignored another (T), (B) Same stimuli as in (A), but the ineffective stimulus (T) was placed outside the RF (adopted from Moran, Desimone, 1985).

the properties of a particular object out of the many that is represented in their response rate (Moran, Desimone, 1985).

Moreover, attention was demonstrated to decrease the width of the tuning function of visual neurons (Martinez-Trujillo, Treue, 2004; Spitzer, et al., 1988). Sharpening the tuning function of neurons allows a better discrimination between similar visual stimuli. Furthermore, some previous electrophysiological studies have demonstrated that neurons in the macaque lateral prefrontal cortex (LPFC), specifically area 8a, show strong response modulation with attention. Their findings reflected an enhancement of neuronal responses to behaviorally relevant stimuli (i.e. target) relative to irrelevant stimuli (i.e. distractor) (Everling et al., 2002; Lebedev et al., 2004).

A recent study by Lennert (Lennert, Martinez-Trujillo, 2011) has shown that such a modulation in LPFC correlated with the behavioral performance of the animals; specifically, the suppression of distractor information is more pronounced when animals can better focus their attention on a target while ignoring a distractor.

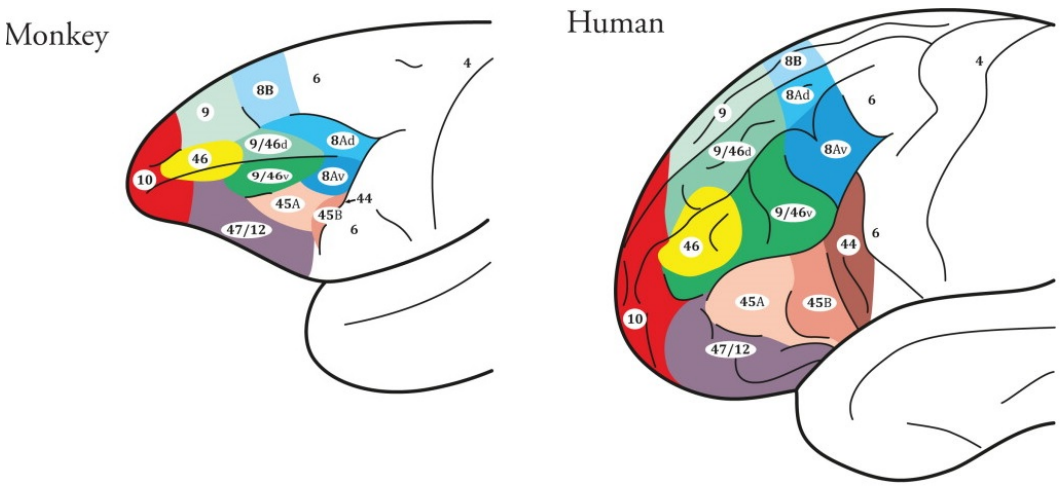

Figure 1.2: **Comparative Cytoarchitectonic Macaque Monkey and Human Prefrontal Cortex**
Architectonic of Lateral prefrontal cortex of (left) macaque monkey and (right) human brain (Adopted from Petrides et. al, 2012).

In conclusion, studies of the neural signal suggest that these signals play an important role in understanding how the brain filters attentional information of behaviorally relevant signals from irrelevant ones.

1.3 Brain Region Involved in Selective Attention

Scientists have long believed that the prefrontal cortex (PFC) plays an important role in control of cognitive processes such as working memory (Goldman-Rakic, 1987; Miller et al., 1996), response strategies (Genovesio et al. 2006), and rule learning (Asaad et al. 1998; White, Wise 1999) (Figure 1.2). More recent studies of humans with lesions of PFC described the effects of lesion as a disruption of 'executive function' and, in particular, attention (Szczepanski, Knight, 2014; Gregoriou, 2014; Rossi, 2007). All of the aforementioned high-level behavioral functions suggest that PFC neurons might modulate responses in sensory areas according to attention and task demands.

Evidences from neurophysiology also justify that patterns of neuronal activity in subregions of PFC are correlated with attentional states (Everling et al., 2002; Lennert, Martinez-Trujillo, 2011). However, a similar response pattern is shown by neurons in other brain areas such as the frontal eye fields (FEFs) (Thompson, Bichot, 2005; Schal 2002), area lateral intraparietal (LIP) (Ipata et. al. 2009), and the superior colliculus in the brainstem (Fecteau, Munoz, 2006). A recent study has demonstrated that during voluntary allocation of attention to a visual target in the presence of distracters, dorsolateral prefrontal cortex (dlPFC) and FEF neurons modulate their firing rate in presence of target prior to neurons in area LIP (Buschman, Miller, 2007). In addition, the FEF shifts the attention toward a target location, regardless of whether the target is present or not, whereas the dlPFC represents the current target location (Buschman, Miller, 2009).

Taken together, these investigations suggest the general hypothesis that attentional signals may emanate first in the prefrontal cortex and then propagate throughout the rest of the brain. In this perspective, PFC is one of brain region involved in the top-down control of attention (Buschman, Miller, 2009). Because the PFC is thought to be one of several brain regions that is involved in attentional network, a question remains as to which attentional functions are dependent on it . Here, we suggested two experiments in which we investigated the role of PFC in splitting visual attention across both hemifields and within one hemifield.

1.4 Research Aims

Attention is known to affect behavioral performance depending on the spatial arrangement of visual items (targets and distractors). Behavioral performance improves strongly when targets and distractors are presented bilaterally compared to unilaterally (Carrasco et al., 2006; Fuller et al., 2008). One plausible explanation for this effect is that anatomically separated contralateral and ipsilateral visual information processing might result in different neuronal computations for bilateral versus unilateral presentations of objects (Figure

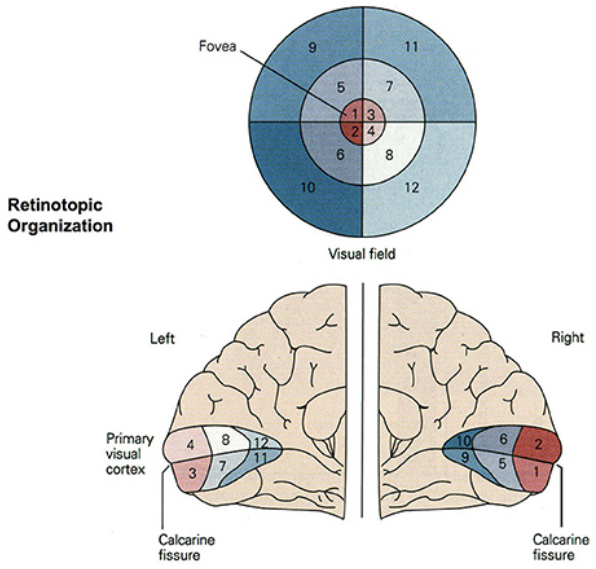

Figure 1.3: **Retinotopic Mapping**
Retinotopic organization of the primary visual cortex. Up to 50% of the primary visual cortex processes foveal signals (cortical magnification). Signals from the top left of the visual field are mapped to the bottom right of the visual cortex (contralateral) (Adopted from Paulun L. et. al, 2018).

1.3).

These anatomical constraints of visual hemifields may affect the attentional mechanisms that filter target from distractor signals more strongly across hemifields than within one hemifield (Alvarez et al., 2012; Delvenne and Holt, 2012; Störmer et al., 2014; Walter et al., 2015). However, neurophysiological evidence in favor of this effect remains scarce.

Aim: *Determine neurophysiological correlate of the behavioral anisotropy observed during attending to targets and distractors in different vs same hemifields.*

Some previous work has given credence to the hypothesis that there are independent processing resources for contralateral and ipsilateral stimuli – both in humans (Vandenberghe et al., 2000; Störmer et al., 2014) and non-human primates (Buschman et al., 2011; Matsushima et al., 2014) across a variety of tasks probing different cognitive mechanisms. Matsushima and Tanaka (2014) performed single-unit recordings in PFC while monkeys

remembered the spatial location of one or two stimuli. They found reduced neuronal activity when two stimuli were presented within the same hemifield as compared to when they had to remember either one location or two locations distributed across the visual hemifields. Buschman and colleagues (2011) recorded single units from PFC during a match-to-sample task and reported decreased behavioral performance as well as impaired information coding when objects were added in the same hemifield as the target.

Some studies have compared responses of neurons in early visual areas to stimuli positioned within the receptive field (RF) (usually always in the same hemifield), and one inside and another outside the RF (in different visual hemifields) (Treue and Martinez-Trujillo, 1999; Spitzer and Desimone, 1998). The attentional modulation of responses in the former situation is much stronger than in the latter. This, however, does not explain the results of behavioral studies and further suggests that the explanation of the between vs. within hemifields effect will not be found in early visual areas with a single hemifield representation of the visual environment.

A more plausible hypothesis is that the neural basis of the effect is found in areas where neurons have a bilateral representation of the visual field. One such area is the lateral prefrontal cortex (LPFC). Some studies have previously demonstrated that neurons in the macaque LPFC, specifically the area around the arcuate and principal sulcus (8a), show strong response modulation with attention (Everling et al., 2002; Lennert et al., 2011). Such a modulation is correlated with the behavioral performance of the animals; specifically, the suppression of distractor information is more pronounced when animals can behaviorally better focus attention on a target while ignoring a distractor (Lennert et al., 2011). This suggests that neural activity in the LPFC is causally related to the effects of attention on information processing in the brain. Moreover, different from early visual areas, the LPFC has a bilateral representation of the visual field (Lennert et al., 2013; Tremblay et al., 2015), which can facilitate dynamic competitive interactions between neurons representing stimuli within the same as well as different hemifields. One possible scenario is

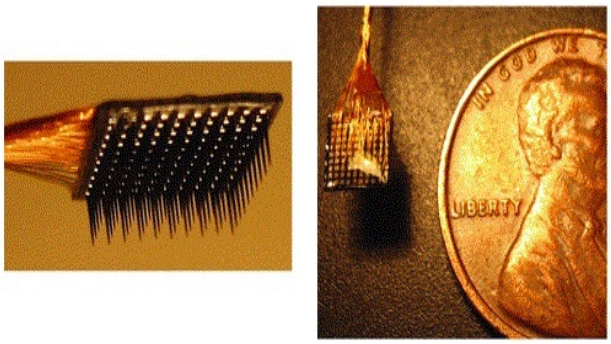

Figure 1.4: **Utah Multielectrode Array**

(left) A 10×10 multielectrode Utah array; (right) The array, closeup, and perspective with a penny (Adopted from Kelly, 2007).

that such competitive interactions are more effective between neurons holding across relative to within hemifield representations of potential targets and distractors.

To test this hypothesis, we simultaneously recorded the activity of neurons in area 8A, which is a cytoarchitectonically defined granular region of the LPFC, of two macaque monkeys by using a 10×10 multielectrode array (Utah multi-electrode array-96 channels, Blackrock Microsystems LLC, Utah, USA) (Figure 1.4).

We recorded activity while the animals covertly allocated attention to one stimulus (the target) and ignored a second stimulus (the distractor). The stimuli were presented one to the left and the other to the right of a fixation point (across hemifields) or both on the same side relative to the fixation point (within hemifield).

To compare our results with later behavioral studies, we looked at behavioral performance of animals in both tasks. Specificity, to explore how the neural response affects performance, we analyzed neural data in three different approaches: 1) single neuron 2) pairs of neurons and 3) neural ensemble approach in both task. Next chapter contains a comprehensive explanation about the experiment and mathematical methods that were used to analyze the data. In chapter 3, we will show behavioral and neural results. Last chapter includes overall discussion about results.

Chapter 2

Materials and Methods

2.1 Animals

Two adult male rhesus monkeys (Macaca mulatta, R: 9.7 kg; S: 10.2 kg) participated in the experiments. All animal procedures complied with the Canadian Council of Animal Care guidelines and were approved by the McGill university's animal care committee's regulations. During the training and testing periods, the animals received their minimum daily amounts of fluids so that they were motivated to perform the tasks. We also gave the animals fresh fruits and vegetables as supplements when finishing a session. Body weight, water intake, mental and physical well-being were monitored on a daily basis. None of the animals were sacrificed for the purpose of this study.

2.2 Surgical Procedures

The surgical operations were carried out under general anesthesia using isoflurane administered through endotracheal intubation. The animals were implanted with titanium head posts used to restrain head motion. We chronically implanted a 10×10 multi-electrode array (96 channels, Blackrock Microsystems LLC, Utah, USA) in each monkey's left LPFC. The array was positioned on the cortical surface anterior to the knee of the arcuate sulcus and caudal to the posterior end of the principal sulcus, known as area 8a in the macaque monkey (Petrides et. al., 2012) (Figure 1.2).

2.3 Electrophysiological Recordings

We recorded from all 96 channels from the left LPFC of both animals. Data were recorded using a Cerebus Neuronal Signal Processor (Blackrock Microsystems LLC, Utah, USA) via a Cereport adapter. After $1\times$ amplification in the head stage (ICS-96), the neuronal signal was band-pass filtered (0.3 Hz- 7.5 kHz) and digitized (16) at a sample rate of 30 kHz. For each channel, spike waveforms were detected by manually thresholding (~ 4 times the root mean square of the noise amplitude) the digitally high-pass filtered (250 Hz/4 pole) raw voltage trace. The extracted spikes and associated waveforms were sorted offline using both manual and semi-automatic techniques using OfflineSorter (Plexon Inc, TX, USA) and Matlab (MathWorks, Natick, MA, USA). We made no assumptions as to whether the recorded units were same or different from day to day (units and neurons are identical in this manuscript)

2.4 Experimental Setup

To begin a trial, the monkeys fixated on a central point on the screen, located approximately 57 cm in front of them and pressed a lever. The experiment consisted of two classes of attentional conditions: Across hemifield condition and within hemifield condition comprising two random dot pattern (RDP) located equidistant from the center of the screen. The position of the RDPs depended on the condition appeared at two different locations; the left and right of the fixation point (across condition) or both in the same side of the fixation point (within condition). In a given recording session, the animals completed several hundred trials, of across hemifield or within hemifield conditions. We totally recorded 4 sessions of across condition (5 sessions in monkey S) and 4 sessions of within condition (2 sessions within right and 2 session within left hemifield).

2.4.1 Task

The animals initiated a trial by keeping gaze within a 2° diameter window (4° in monkey S) centered on a small fixation spot ($0.24^{\circ 2}$). Gaze position was monitored using an infrared video-based eye tracker (EyeLink 1000, SR Research, Ontario, Canada). After a 353 ms fixation period, two moving RDPs appeared at two different locations. The position of the RDPs depended on the condition, either the left or right of the fixation point (across condition) or both in the same side of the fixation point (within condition). The patterns were composed of white dots on a dark background that moved either up (0°) or down (180°) relative to the vertical. After a variable interval (294, 471, or 647 ms) following the RDPs' onset, both patterns changed to different colors (e.g., one to green and the other to red). The task for the animals was to identify one of the two RDPs as the target based on its color and covertly attend to it while ignoring the other (the distractor). After 706 ms, the color was removed and the RDPs returned to white. The animals had to maintain attention on the target and wait between 753 ms to 1600 ms for a brief motion direction change in the target stimulus (118 ms duration, change was 32° clockwise from the current direction) and release the button within 100 ms - 650 ms (Figure 2.1).

In 50% of the trials, the distractor changed motion direction before the target. In those trials, the monkey had to keep holding the lever until the target changed. Which of the two colors indicated a target was based on an ordinal color-rank rule the monkey had learned over the training sessions (turquoise $>$ red $>$ blue $>$ green $>$ pink $>$ grey, see also Lennert & Martinez-Trujillo 2011; 2013). Each correctly performed trial was rewarded with a drop of juice. A sequence of correct trials yielded a slight increase in reward size. Trials in which the monkey responded to the distractor change (false alarms) or did not respond to the target change within the reaction time window (misses) or broke fixation before the end of a trial (fixation breaks), were terminated without reward. The different trial types were presented in random sequence. Only correctly performed trials were included in the analysis unless otherwise indicated.

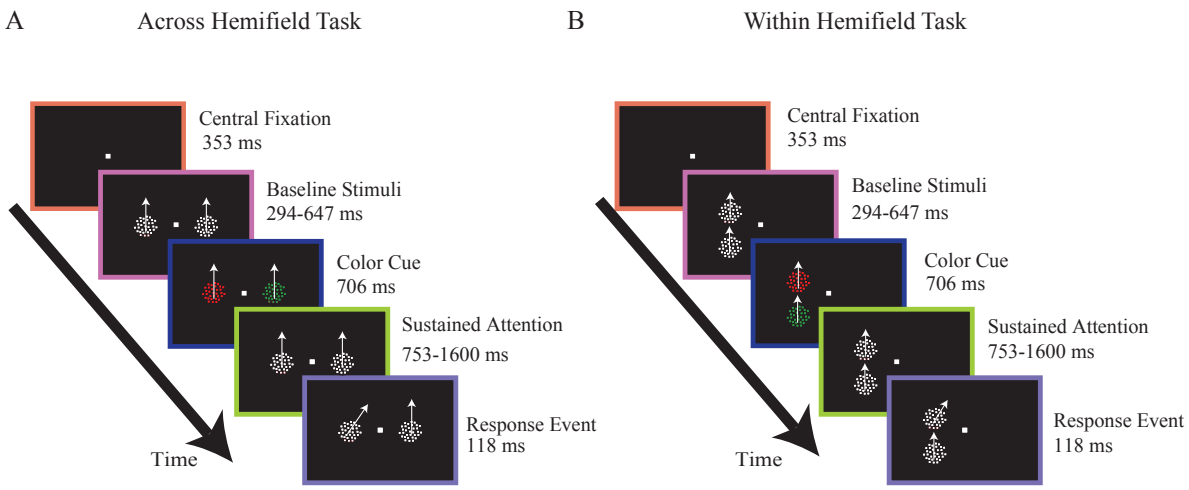

Figure 2.1: **Behavioral Task**

(A) Example trial of the across task with stimuli distributed the left and the right visual fields. (B) Example trial of the within task with both stimuli in the ipsilateral of recording side (left hemifield).

2.4.2 Visual Stimuli

The stimuli were back projected on a screen using a video projector (NEC WT610, 1024×768 pixel resolution, 75 Hz) and custom-made software running on an Apple G4 Power PC. The animals viewed the screen at a distance of 57 cm ($1cm = 1^\circ$ of visual angle). The stimuli were generated by plotting colored dots (white, $76.39\ cd/m^2$; grey, $10.83\ cd/m^2$; pink, $22.68\ cd/m^2$; green, $11.26\ cd/m^2$; blue, $10.96\ cd/m^2$; red, $8.92\ cd/m^2$; turquoise, $44.14\ cd/m^2$) on a dark background (black-gray, $0.74\ cd/m^2$) with a density of three dots per degree^2 within a circular stationary virtual aperture. All dots within one random dot pattern (RDP) moved coherently at a speed of 15°/s and were replotted at the opposite side when they crossed the border of the aperture. The radius of the aperture was 4°. In the across-hemifield condition, the RDPs' centers were 8° away from the fixation spot and the two stimuli were 16° apart, whereas in the Within-hemifield condition, their centers were also presented at 8° eccentricity but on the diagonal, which made the two stimuli

11.33° apart. We chose the differences in distance between the stimuli to keep eccentricity constant, which had an effect on the animals' performance when designing the experiments (Whitney et al., 2011; Rovamo et al. 1982).

2.5 Data Analysis

Analysis of spike data (firing rates) and statistical tests were performed using MATLAB. Our analyses were computed for different epochs. A 350 ms window during fixation period and a 500 ms window during baseline (150 ms after fixation offset-650 ms after fixation offset), cue (150 ms after color onset – 650 ms after color onset) and post-cue/sustained attention (200 ms after color offset – 700 ms after color offset).

We recorded the response of 856 neurons in monkey R (525 over 4 sessions of the across condition and 331 over 4 sessions of the within condition) and 789 neurons in monkey S (556 over 5 sessions of the across condition and 233 over 4 sessions of the within condition). We excluded neurons with a firing rate less than 0.1 Hz.

2.5.1 Neuronal Selectivity

We determined neuronal selectivity by performing a one-way analysis of variance (ANOVA) with target location as a factor using mean activity of each neuron within a 100 ms window starting from each epoch onset and slid along the trial in steps of 10 ms independently for four different epochs. If the neuron revealed a significant effect of target position ($p < 0.05$) in at least five consecutive time bins, it was classified as a target selective unit. The position of the target (left or right in across condition and up or down in within conditions) at which the unit produced stronger response (two sample t-test $p < 0.05$) was considered the neuron's preferred location (Lennert et al. 2011).

We calculated the proportions of location-selective cells in the entire population in the different periods for each task. We compared the proportions between periods and conditions using a Chi-Square (χ^2) test. In order to determine whether these proportions were different

from those expected by chance, we compared them to those obtained using a randomization procedure (chance level). For the randomization procedure, we used the same trials and units as in the original data but shuffled the trial orders before running the analyses.

2.5.2 Spike Density Functions

The activity of selective neurons was plotted as mean spike density functions (SDF) over trials, generated by convolving the spike train with a Gamma kernel function (growth parameter 1 ms and decay parameter 20 ms) (Hanes et al., 1996). We normalized SDF for each neuron by the maximum firing rate of the neuron.

2.5.3 Neuronal Sensitivity

To quantify the ability of single neurons to discriminate between targets and distractors, we used the sensitivity index, $d^{'}$, which was calculated as follows:

$$d_j^{'} = \frac{|fr_1 - fr_2|}{\sqrt{0.5({\sigma_1}^2 + {\sigma_2}^2)}},$$

where $d_j^{'}$is sensitivity index for neuron j, fr_i is mean response of neuron j to the two possible target locations $i(i = 1, 2)$ and σ_i is variance of the responses over target location i. The $d^{'}$ values were calculated for a 100 ms window slid in steps of 1 ms along the spike density function for each neuron. We also shuffled the trial order 50 times for each neuron and computed $d^{'}$ to obtain "chance level" sensitivity. A permutation test was used to compare the distributions of $d^{'}$ values in each bin.

2.5.4 Neural Discriminability Index

The measure used to quantify the ability of the pairs of neurons to discriminate target location from distractor location is receiver operating characteristic (ROC) curve for the distribution of neural responses. Our metric differs from ROC in that it is based on projections

of the population response onto a specific attention axis (Moreno-Bote et al., 2014; Mayo et al., 2015). To build the attention axis between two neurons, neuronal responses in each trial to the stimulus presentations were plotted as a point in a 2-dimensional space where each neuron considered as one axis. The line connecting the means of neuronal responses in each attention location was defined as the attention axis. Neuronal responses were then projected onto the attention axis. The projections were scaled for each dataset so that a projection of 1 was equal to the mean response to target in left/up and -1 was the mean response to target in right/down. We calculated distributions of projections for each target location. Thus, the discriminability index (DI) of two neurons is simply,

$$DI = \frac{Separation\ of\ distribution\ of\ neural\ responce\ for\ each\ target\ location(=2)}{average\ Standard\ Deviation\ of\ distributions}$$

.

DI depends on both the separation (signal) and the spread (noise) of distribution functions. Discriminability is made easier either by increasing the separation (stronger signal) or by decreasing the spread (less noise). The DI values were computed in 50 ms non-overlapping sliding windows. Neurons with firing rates less than 0.1 in at least one bin were excluded from analysis. We also shuffled the trial order 50 times for each neuron and computed DI to obtain 'chance level'. A permutation test was used to compare the distributions of DI values in each bin.

2.5.5 Population Decoding of Attended Location

2.5.5.1 Optimized Neural Ensemble

We decoded the information carried by a neural ensemble using a linear decoder. We used a L2-regularized logistic regression (LR) (Fan et al., 2008) to decode the attended location from increasingly larger ensembles. The details of the ensemble building procedure have been described elsewhere (Leavitt et al. 2017). Briefly, we started our ensemble of $n = 1$

with the most informative single unit (based on all units' individual decoding performance) and then iteratively paired it with all remaining units until we identified the unit that maximized the decoder's performance and then added it to the ensemble ($n = 2$). Starting again with the best pair, we identified the best trio by repeating the same procedure, and the best quartet, and so forth. We repeated this procedure 100 times.

We normalized the firing rate of each unit across all trials by subtracting the mean and dividing by the standard deviation (z score). These two parameters (mean and standard deviation) were estimated from the training set and applied to both the training set and the testing set.

To assess the accuracy of the decoder, we used a cross-validation technique: The decoder was trained on 80% of the trials and then tested on the remaining 20% of trials (5-fold cross-validation). The LR was iteratively trained and tested on different subsamples of the trials until each trial was included in the training set at least once. Furthermore, we balanced the number of trials between the conditions by determining the sample size. Shuffled decoding performance (i.e., chance level) was obtained by randomizing the trial order 100 times. When testing the LR on such trials, we obtained the chance performance, which approximates $100 \times (1/N)$: N being the number of possible labels (e.g. $N = 2$).

We integrated the firing rate of each unit within the whole population using several time windows centered at different epochs. We chose a 400 ms time window during cue epoch because it yielded good decoding accuracy (Figure 4.2). Therefore, we computed ensemble decoding accuracy over a 400 ms windows during cue epoch (300 ms after cue onset-700 after cue onset) for different ensemble sizes. We investigated whether the maximum decoding performance and corresponding ensemble size differed between conditions by comparing the maximum accuracy and corresponding ensemble size.

We also computed a mean decoding accuracy for the ensemble of neurons with the maximum decoding accuracy, the optimized ensemble, using a 400 ms window sliding by 100 ms over the time course of the experiment for each condition.

2.5.5.2 Generalized Ensemble Performance

We estimated the generalizability and stability of our optimized ensemble by using two cross validation steps. Without the second cross validation we would only have information on how our model performed for our sample data. Ideally, we wanted to see how the model performed when we have novel data in terms of accuracy of its predictions. Hence, we broke the data up into two partitions; 80% for training and 20% for validation. We used 5-fold cross validation on the training set and split it into training and test sets and applied the same decoding procedure that has been described in a previous section to find our fitted model. Then we ran the obtained model on unseen data (validation data set) and found the decoding accuracy.

2.5.6 Correlation Structure

We computed noise correlations (rnoise) by z-scoring the firing rate of each neuron for each unique condition, thus removing any possible changes in firing rate due to different responses to different stimuli. We then computed pairwise Pearson's correlation coefficients between the z-scored spike counts.

We assessed the impact of correlations between pairs of neurons on optimized ensemble decoding accuracy by removing noise correlation between pairs. To destroy noise correlation structure, we applied a randomizing procedure in which the trial order in each target location (e.g. target in left) was shuffled for each neuron individually, thus breaking up the simultaneity of recordings and eliminate noise correlation. This shuffling procedure was repeated 100 times. The difference between decoding performance with and without correlations was assessed using a paired sample Student's t-test.

Chapter 3

Results

3.1 Behavioral Performance

We compared the animals' correct responses, false alarms, and miss rates between the three conditions (Figure 3.1). There was a significant decrease in the proportion of corrects trials in both monkeys in the within relative to the across condition (monkey R: across condition, mean [M]=90.86%, standard deviation of mean [SD]=5.27%; within left condition, M=84.96%, SD= 9.81%; within right condition, M=84.71%, SD=5.% monkey S: across condition, M=65.19%, SD=1.23%; within left condition, M=47.36%, SD= 0.64%; within right condition, M=48.69%, SD=0.38%; χ^2 test $p < 10^{-3}$). Interestingly, when looking at the kinds of errors the animals made, the proportion of responses to the distractor (i.e., false alarms) and the proportion of misses (i.e., no responses to a change in the target) increase significantly in within conditions relative to across condition in both monkeys (χ^2 test $p < 0.05$) (Table 3.1). In addition, there was no significant behavioral performance change between within left and within right conditions.

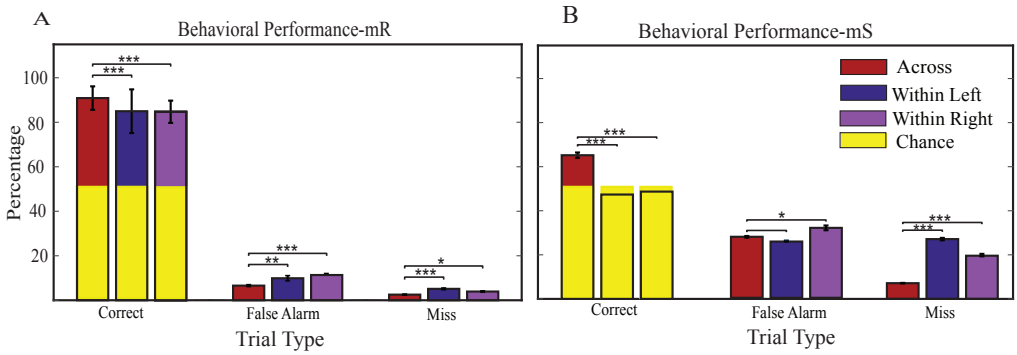

Figure 3.1: **Behavioral Performance**

Percentage of correct, false and miss trials for the across task (red bars), the within left task (blue bars) and the within right task (magenta bars) for both monkeys (A: monkey R, B: monkey S). Yellow bars indicate chance level. Error bars represent standard deviation across sessions. Asterisks mark significant differences in mean performance (χ^2 test * $p < 0.05$, **$p < 10^{-2}$ and *** $p < 10^{-3}$).

Consistent with previous research (Carrasco et al., 2006; Fuller et al., 2008), these results indicate that attentional filtering is less effective when the target and distractor are in the same hemifield as compared to when they are distributed across hemifields. In addition, performance of one animal in within condition task was not above chance level. So, the neural data from this animal was not used for the analyses of single cell responses. In the rest of this thesis, we discuss data from monkey R only.

A

Proportion of Responses-mR

Trial Types	Stat.	Across	Within Left	Within Right	Chi2 -Test
Correct	M	90.86%	84.96%	84.71%	p<0.001
	SD	5.27%	9.81%	5.%	
False Alarm	M	6.58%	9.89%	11.35%	p<0.01
	SD	0.43%	1.18%	0.05%	
Miss	M	2.54%	5.14%	3.93%	p<0.01
	SD	0.1%	0.27%	0.19%	

B

Proportion of Responses-mS

Trial Types	Stat.	Across	Within Left	Within Right	Chi 2-Test
Correct	M	65.19%	47.36%	48.69%	p<0.001
	SD	1.23%	0.64%	0.38%	
False Alarm	M	27.68%	25.52%	31.73%	p<0.05
	SD	0.35%	0.58%	1.1%	
Miss	M	7.12%	27.12%	19.58%	p<0.05
	SD	0.14%	0.54%	0.07%	

Table 3.1: **Proprtion of Responses**

Mean (M) and standard devation (SD) of correct, false and miss trials for the across, the within left and the within right task for (A) monkey R, (B) monkey S. p is significant differences in mean performance of across task and within tasks (χ^2 test).

3.2 Single Unit Selectivity

We examined whether recorded unit's responses were modulated by the location of the target stimulus using a one-way ANOVA (see methods). Figures 3.2D & E show mean firing rate of two examples of location-selective units. Figure 2D shows units that responded more strongly when the target location was on the left side of the fixation point (ipsilateral to recording side) in the across condition (target in the left side, M=0.6, SD=0.03; target in the right side, M=0.51, SD=0.03, paired t test $CI = 0.0806 - 0.0857$, $p = 0$). Figure 3.2E shows units that responded more strongly when the target was presented below the fixation point in the within left condition (target above the fixation point, M= 0.42, SD=0.05; target below the fixation point, M=0.49, SD=0.05, paired t test $CI = 0.0691 - 0.0735$, $p = 0$).

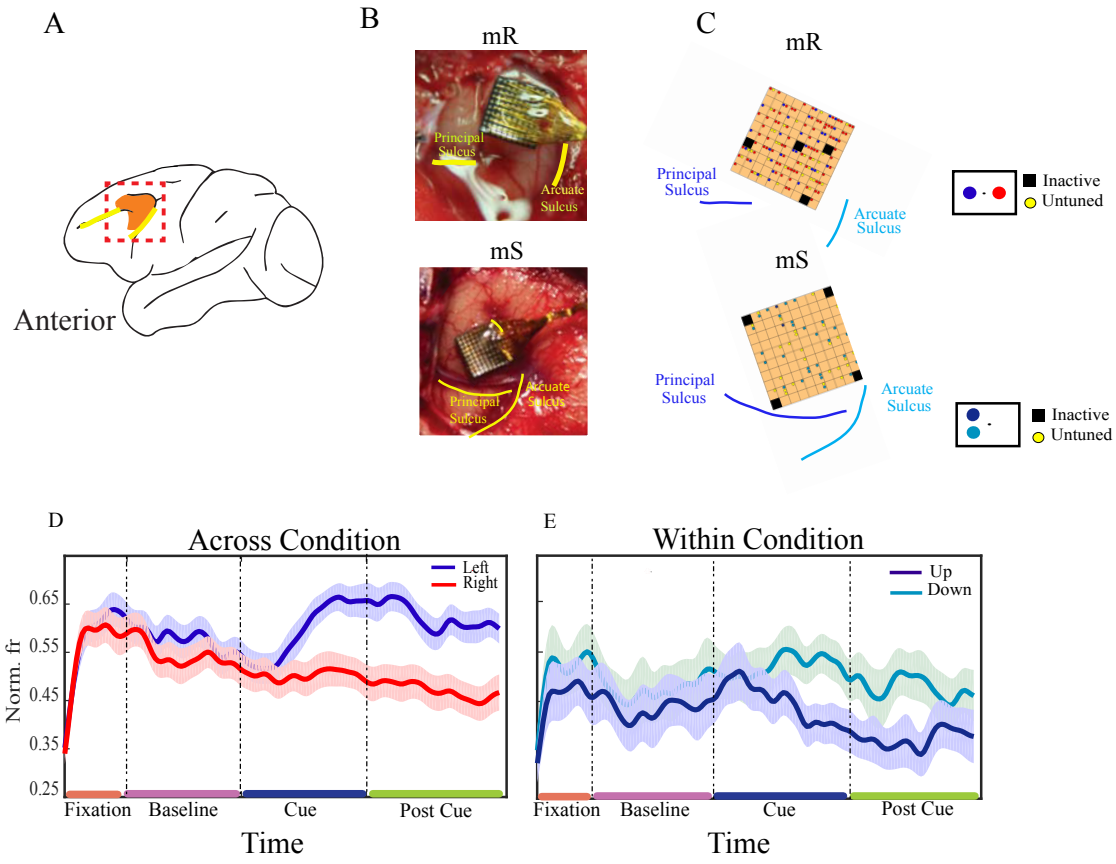

Figure 3.2: **Array Location and Electrophysiological Recording**

(A) Schematic of a macaque brain with area 8a of LPFC highlighted (B) Anatomical location of the multielectrode array implanted in monkey R (top) and monkey S (bottom). Photographs were taken during the implantation procedure. Principal and arcuate sulci are indicated. (C) Precise location of implants in monkey R and S according to intraoperative photography. Colors code for the spatial attention tuning of the multiunit recorded at each electrode site. (D-E) Mean Normalized responses of tuned units to the different target positions from monkey R recorded during (D) the across condition (ipsilateral target: light blue, contralateral target: light red) and (E) the within condition (target up: light blue, target bottom: dark blue) as a function of time. Shading represents SEM ($\pm$) at each time point. Colored horizontal lines represent different time epochs of experiment: fixation (orange), baseline (magenta), cue (dark blue) and post cue (light green) which are consistent in all figures.

Similarly, we compared the proportions of location-selective units for four different task epochs in the across, within left, and within right conditions (Figure 3.3). Figure 3.3A shows a significant increase of proportion of tuned units in cue (across, M=0.40, SD=0.02; within left, M=0.21, SD=0.07; within right, M=0.10, SD=0.04) and post-cue (across, M=0.36, SD=0.02; within left, M=0.20, SD=0.07; within right, M=0.09, SD=0.04) periods compared to the fixation period (across, M=0.05, SD=0.002; within left, M=0.04, SD=0.005; within right, M=0.04, SD=0.01) for three conditions (χ^2-test, $p < 10^{-3}$ for the across and within left condition and $p < 0.05$ for within right condition). Figure 3.3B exhibits the proportions of location-selective units from cue (across, M=0.40 ,SD=0.02; within left, M=0.21, SD=0.07; within right, M=0.10, SD=0.04) and post-cue (across, M=0.36, SD=0.02; within left, M=0.20, SD=0.07; within right, M=0.09, SD=0.04) period which were significantly different between conditions (χ^2-test, $p < 10^{-3}$). In Figure 3.3C, we examine whether the proportions of selective cells were relatively stable over sessions. Interestingly, from one session to the next, there were slight differences between proportions of tuned units over epochs, but overall there were very similar distributions of tuned units over epochs. This suggests that the selectivity was stable over recording sessions.

Together, our results indicate that single units in LPFC are significantly less selective for the attended location in the within relative to the across condition.

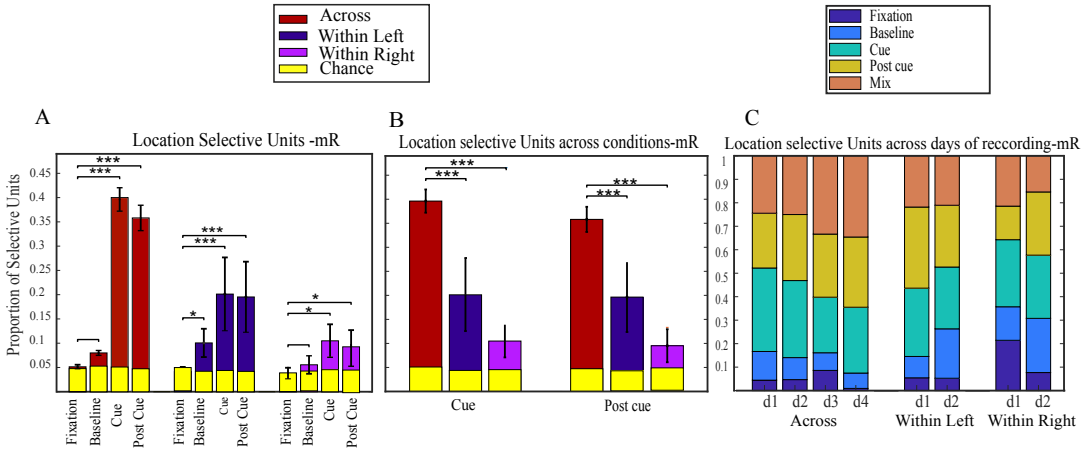

Figure 3.3: **Single Unit Selectivity**

(A) Proportion of location-selective units (one-way ANOVA with factor target location ($p < 0.05$)), for four different condition periods in the across condition (red bars), the within left (blue bars), the within right (magenta bars) and chance level (yellow bars). Error bars represent SEM ($\pm$) over recording sessions. Asterisks mark significant differences in mean proportion (χ^2-test; * $p < 0.05$, ** $p < 0.01$, ***$p < 0.001$). (B) Comparison of proportion of tuned units in cue and post cue epochs across three conditions (C) Proportion of tuned units in each recording sessions to see whether the distributions of tuned units were approximately stable over time.

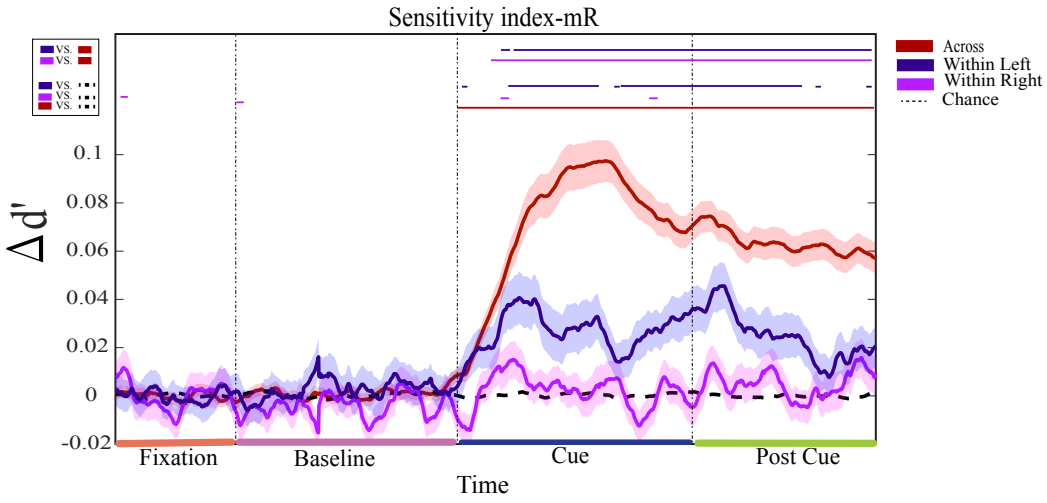

Figure 3.4: **Sensitivity Index**

Average $d^{'}$ as a function of time for location-selective units recorded during across (red), within left (dark blue) and within right (magenta) conditions. Shading represent SEM ($\pm$). Dashed black line represents chance level. Horizontal lines on top indicate at which time bins $d^{'}$ was significantly different from chance level and across condition (Permutation test, $p < 0.05$).

3.3 Single Unit Sensitivity

We computed an index of sensitivity ($d^{'}$) for the location-selective units (tuned units) in 100 ms bins with 1 ms sliding windows to assess whether single neurons could discriminate between targets and distractors in three conditions. Single-neuron sensitivity was above chance level, which was obtained from shuffled trial orders (50 shuffles), in many bins in three conditions, as indicated by the correspondingly colored horizontal lines (Permutation test, $p < 0.05$) (Figure 3.4). $d^{'}$ was significantly stronger in the across condition than in the within conditions starting from color cue onset and remaining until the end of the post-cue period (Permutation test, $p < 0.05$).

Overall, these results indicate that location-selective units in LPFC are less sensitive when discriminating targets from distractors in the within relative to the across condition.

3.4 Discriminability Index

We investigated the ability of different pairs of neurons to discriminate the target from the distractor in each condition by computing a discriminability index (DI) between pairs of tuned-tuned, tuned-untuned, and untuned-untuned neurons. The DI values were computed in nonoverlapping 50 ms sliding windows. Neurons with firing rate less than 0.1 in at least one bin were excluded from analysis. We also shuffled the trial order 50 times for each neuron and computed DI to obtain 'chance level'. A permutation test was used to compare the distributions of DI values in each bin. DI between tuned-tuned and tuned-untuned neurons were stronger in across condition than within left and within right conditions (Figure 3.5A-B). DI increased from fixation to color cue and remained almost constant in post-cue period in across condition but in within left and within right conditions this pattern was less distinct indicating fewer tuned units in those conditions (Figure 3.3A). DI between untuned-untuned pairs was not above chance-level (permutation test, $p > 0.05$) (Figure 3.5C).

We used a microelectrode array in which electrodes were at fixed positions (see methods). We took advantage of this and measured how distance between tuned neurons in a pair modulated the DI, ranging from 0.4 to 4 mm apart. Considering that the width of a prefrontal cortical column is about 0.7–0.9 mm (Bugbee et. al, 1983), this analysis can reveal functional interactions between neurons located within the same or in nearby cortical columns. Our results showed that DI decreased as distance increased in the across condition in cue and post-cue epochs ($0 < r < 0.8$ mm, M=0.18, SD=0.04; $r > 2.4$ mm, M=0.16, SD=0.03, Wilcoxon rank sum p=0.001) (Figure 6A). However, this effect was not present in the within left and within right conditions (within left condition, $0 < r < 0.8$mm, M=0.12, SD=0.01; $r > 2.4$mm, M=0.12, SD=0.008, Wilcoxon rank sum $p \sim 0.8$; within

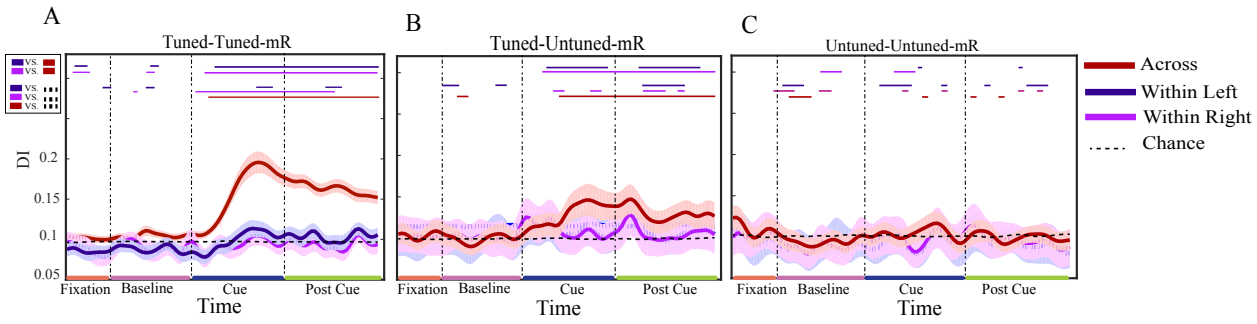

Figure 3.5: **Discriminability Index**

(A-C) Average DI as a function of time between (A) tuned-tuned, (B) tuned-untuned and (C) untuned-untuned units recorded during across (red), within left (dark blue) and within right (magenta) conditions. Shading represents SEM ($\pm$). Dashed black line represents chance level. Horizontal lines on top indicate at which time bins d' was significantly different from chance level and across condition (Permutation test, $p < 0.05$).

right condition, $0 < r < 0.8$mm, M=0.12, SD=0.015; $r > 2.4$mm, M=0.13, SD=0.016, Wilcoxon rank sum $p \sim 0.8$) (Figure 3.6B-C). It might provide a proper explanation that signals from the same visual field are processed highly competitively and averaged through recurrent connections, whereas signals from opposite hemifields are processed almost independently and spared in distinct cortical columns.

Our analysis indicated that pairs of neurons were better able to discriminate target from distractor in the across condition than the within condition, especially pairs with shorter inter-neurons distance. A novel finding of our analysis was that the pattern of DI over the time course of the experiment reflects the ability of pairs of neurons to encode target location.

3.5 Performance of Neuronal Ensembles

Single unit analyses inform us about how a population of independently firing neurons encodes information about a stimulus or behavioral state. However, neurons in the LPFC do not fire independently, as they show correlated variability that can affect information cod-

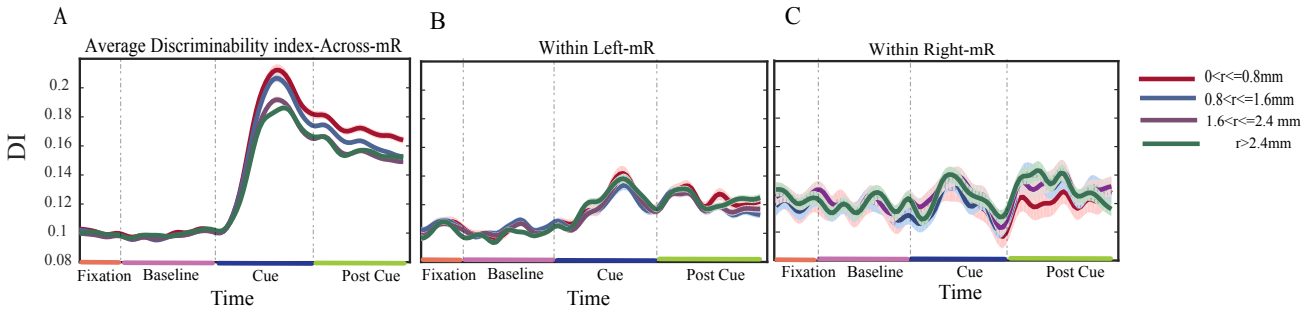

Figure 3.6: **Discriminability Index vs. Interneuron Distance**

(A-C) Average DI as a function of time and interneuron distance (r) in (A) across, (B) within left and (C) within right conditions. Shading areas represent SEM (±).

ing (Tremblay et al., 2015). We have previously used classifiers to determine how neuronal ensembles in the LPFC encode information regarding the focus of attention when considering correlated variability. Here we apply the same methodology (Leavitt et al. 2017; Backen et. al. 2018).

We used a binary, linear classifier – the L2 regularized logistic regression (LR)– to decode target location in the three conditions from the activity of the simultaneously recorded ensembles. The decoder plays the role of a downstream neuron or mechanism that reads out the information from the neuronal ensemble to estimate the target/attended location. We assessed the decoder's accuracy using a cross-validation technique in which it iteratively learned the neural response patterns to the stimulus conditions in 80% of the trials and was then tested on the remaining 20%. We integrated the firing rate of each unit within the whole population using a 400 ms window during cue epoch (300 ms after cue onset-700 ms after cue onset) because it yielded good decoding accuracy (Figure 4.2).

We progressively built neuronal ensembles by starting with the most informative single unit and then iteratively adding units that maximized the decoder's performance (see Methods). To compare with randomly selected units, we performed this analysis for each ensemble size by bootstrapping from all population 100 times. To find chance level, we repeated this

procedure by randomizing the trial order for each neuron individually, thus breaking up the simultaneity of the recordings and the shared trial-by-trial variability in the responses (i.e., noise correlations).

Figures 3.7 shows the ensemble decoding performance in the three conditions. Interestingly, the decoding performance in the optimized ensemble model rose quickly and then plateaued or even slightly decreased as ensemble size increased, suggesting that the entire population of recorded units was not required to reach the maximum decoding performance. The optimized ensemble model had greater accuracy relative to the randomized model. Figure 3.7(A-C) shows the ensemble decoding accuracy was higher for the across condition than for the within left and within right conditions and significantly above chance in all ensemble sizes (Wilcoxon rank-sum test, $p < 0.05$).

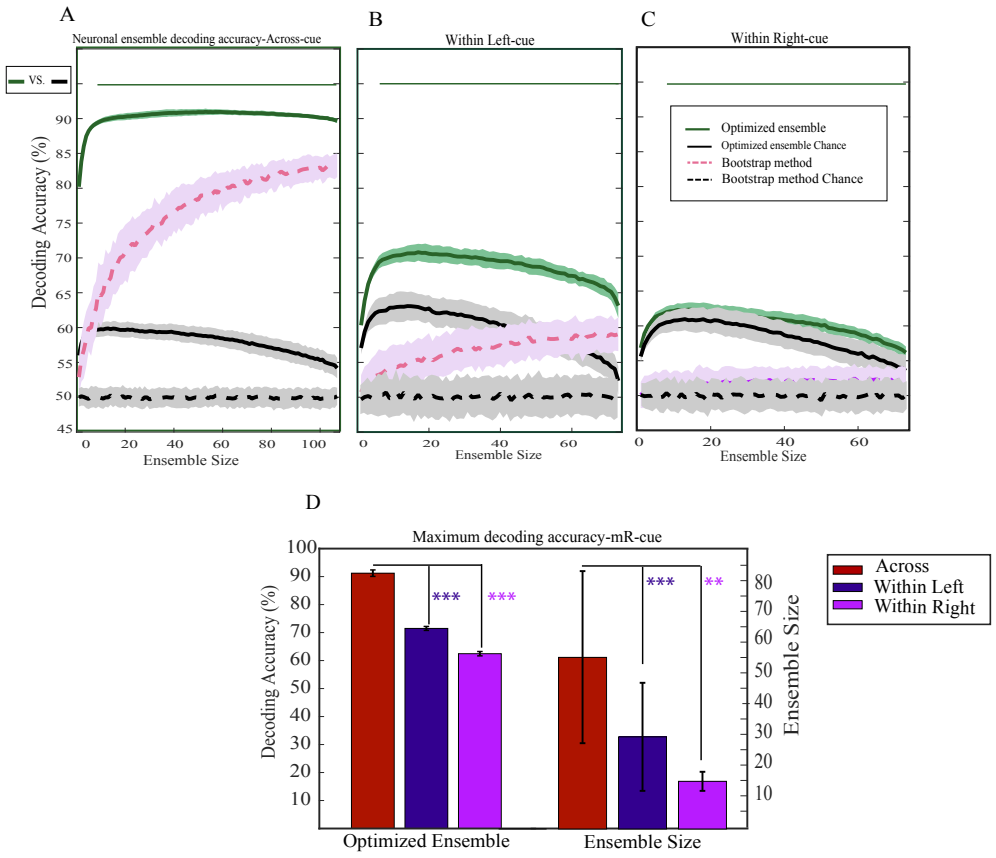

Figure 3.7: **Ensemble Decoding of Target Location**

Decoding accuracy using 400 ms window centered 500 ms after cue onset from increasingly larger ensembles according to optimized method (solid green lines) in the (A) across, (B) within left and (C) within right conditions. Dashed pink lines represent decoding accuracy from random ensembles. Shading indicates SEM ($\pm$) for each ensemble size. The solid black lines symbolize chance performance for optimized ensemble and dashed black lines show chance performance for random ensemble. Horizontal lines on top indicate at which ensemble size optimized ensemble was significantly different from it's chance level (Wilcoxon rank sum $p < 0.05$). (D) Average maximum decoding accuracy (left) and average corresponding ensemble size to maximum accuracy (right) in optimized ensemble over recording sessions. Error bars denote standard deviation across sessions. Asterisks mark (left) significant differences in mean accuracy over recording sessions (two sample t test; *** $p < 0.001$) and (right) significant differences in mean corresponding ensemble size to maximum accuracy over recording sessions (χ^2 test; *** $p < 0.001$, ** $p < 0.01$).

Next, we assessed whether the maximum decoding accuracy and corresponding ensemble size differed between conditions (Fig. 3.7D). In the across condition task, the accuracy of the ensemble after maximum decoding performance was reached was more stable as compared to the within left and within right conditions (across, average maximum accuracy [MA]= 91% , SD=1.15%, average corresponding ensemble size N=55, SD=27.29; within left, MA=71.46% , SD=0.71%, N=29, SD=17.67 and within right, MA= 62.46%, SD=0.78%, N=15, SD=3.5). This result indicated that the across condition had more informative neurons than the within left and within right conditions (χ^2 test , p< 0.01). Furthermore, the latter result suggests that size of the ensemble was not a contributing factor to the changes in decoding accuracy we have observed.

3.5.1 Generalized Ensemble Performance

We estimated the generalizability and stability of our optimized ensemble by using two cross validation steps. Without the second cross validation we would only have information on how our model performed for our sample data. Ideally, we wanted to see how the model performed when we have novel data in terms of accuracy of its predictions (see methods).

Interestingly, the across condition decoding of the validation set was more accurate and significantly above chance than the within conditions decoding (across, MA= 83%, SD=1.12%; within left, MA=55%, SD= 5.1% and within right, MA=50%, SD=3.5%, Wilcoxon rank rest, $p < 0.05$). Moreover, this result shows that there is more stability in neuronal responses in the across condition than in the within conditions (Figure 4.3).

3.5.2 Neural Ensemble Activity

In order to analyze the time course of the neural signals for attentional allocation, we trained and tested the decoder at different time points under three conditions. We used a 400 ms sliding window with 100 ms steps to integrate the firing rate of neurons in three different

neural ensembles 1) the ensembles with maximum decoding accuracy (optimized ensemble) (Figure 3.7), 2) the ensembles with the same size as the optimized ensemble, generated through 100 bootstrap samples (random ensemble) and 3) the full ensemble size in each condition.

The decoding accuracy increased from the end of baseline and reached its maximum in the cue period, then decreased in post-cue in the each conditions. Compared to the random ensemble (brown line), and the full ensemble (green line), the optimized ensemble (magenta line) resulted in higher decoder classification performance which was significantly above chance in the cue epoch in each of the three conditions (Figure 3.8, Wilcoxon rank-sum test, $p < 0.05$). Thus, the optimized neuronal ensembles encode spatial attention information more reliably and do so even when single units were not particularly informative about the decoded feature (target location), as was the case in the within right condition (Figure 3.4).

These results emphasize that LPFC neural ensembles encode information and can select a visual target among distractors within timeframes of a few hundred milliseconds. The latter result implies that using the full ensemble (green line) was not required to produce the highest decoding accuracy. In contrast, the full ensemble generally encoded an equal or greater amount of information in post-cue, which is the sustained attention epoch, relative to the optimized ensemble. The latter results suggest that all neurons in the ensembles may be needed to reach a stationary state (post-cue) that contains more information about external stimuli than an optimized ensemble. However, one must interpet these data cautiously since the differences in decoding accuracy were in general small.

Decoding accuracy was higher in the across condition than the within left and within right conditions at all time points (Figure 3.8). One possibility that may explain the lower performance in the within conditions is that the performance of the optimized ensembles was different depending on the hemifield where the target and distractor were presented. Decoding accuracy of ipsilaterally (within left) and contralaterally (within right) presented

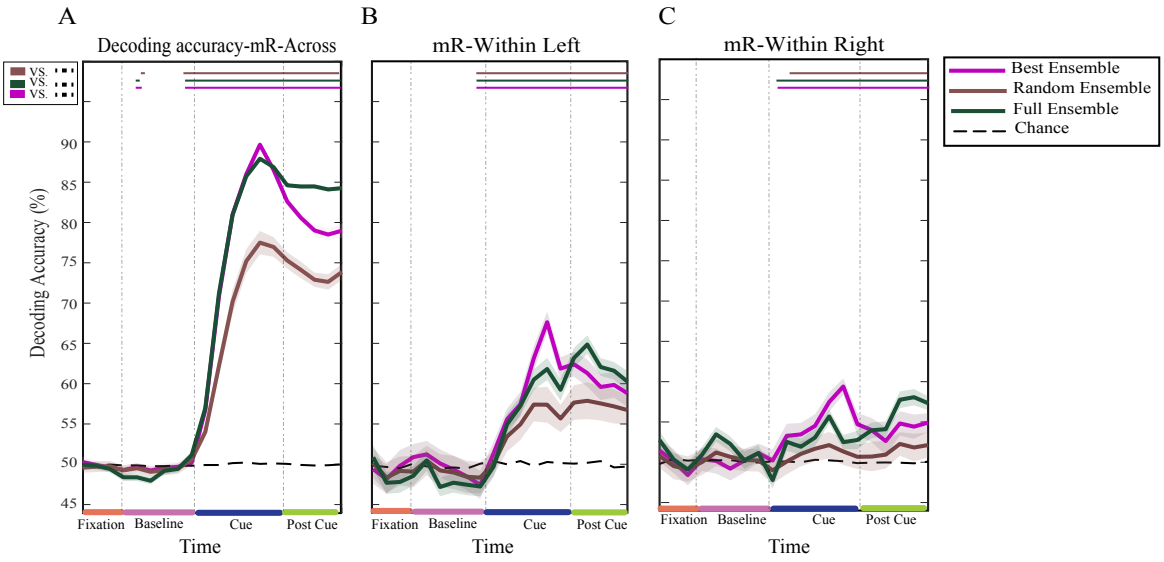

Figure 3.8: **Ensemble Decoding Accuracy vs. Time**

Decoding accuracy using 400 ms window sliding with 100 ms window for optimized ensemble (pink lines), full ensemble size (dark green lines) and random ensemble with same size of optimized ensemble (brown lines) in the across, within left and within right conditions. Dashed black lines represent chance performance. Shading indicates SEM ($\pm$) for each time point. The straight lines at the top indicate statistically significant (Wilcoxon rank sum $p < 0.05$) between ensemble performance vs. chance performance.

stimuli was not statistically different (within left, average maximum accuracy in cue period [MA]=67%, SD=1%; within right, MA=59%, SD=2%, two-sample t-test, $p \sim 0.119$).

Generally, we observed that neural ensembles decoded information from the across condition more accurately than the within conditions. When both stimuli were presented in the same visual hemifield there was a decrease in decoding accuracy, potentially because they represent positive feedback signals between neurons that encode the same visual hemifield. In addition, we found that neural ensembles store more information when the target location is ipsilateral to the recording side rather than when they are contralateral to recording side.

3.5.3 The Effect of Noise Correlations on Performance of Neural Ensembles

One explanation for these results is that noise correlations may have contributed to the observed lower ensemble performance in the within left and within right conditions compared to the across condition. However, whether noise correlations always have a negative effect on the amount of information that can be stored in population activity is still being debated theoretically (Averbeck B. B et al. 2006; Cohen M.R. et al. 2011; Ruff D.A. et al. 2014). It has recently been proposed that combining simultaneous recordings with decoding methods can explain whether noise correlations definitely limit the information coding capabilities of a neuronal population (Arandia-Romero I. et al. 2016; Moreno-Bote et al. 2014). To explore this issue, we removed noise correlations from the optimized ensemble by shuffling the identity of trials belonging to the same trial condition (e.g. target is in the left) for each individual neuron (Tremblay S. et al. 2015).

Removing noise correlations had a different effect depending on the condition. Reducing noise correlation (dashed lines with open circles) slightly improved decoding accuracy in the across condition in cue epoch (M=0.42%, SD=0.93%, $p = 0.32$, $CI = 1.3979 - (-0.5579)$ paired t-test) as well as attention (post-cue) period (M=1.66%, SD=0.82%, $p = 0.0044$, $CI = 0.7901 - 2.5199$ paired t-test). On the other hand, decreasing noise correlation slightly decreased decoding accuracy for ipsilateral and contralateral presented stimuli in cue epoch (within left, M=-0.19%, SD=1.39%, $p = 0.75$, $CI = 1.2636 - (-1.6436)$ paired t-test; within right, M=-0.70%, SD=1.09%, $p = 0.17$, $CI = 0.4412 - (-1.8445)$ paired t-test) and in post-cue period (within left, M=-0.58%, SD=1.4281%, $p = 0.37$, $CI = 0.9237 - (-2.0737)$ paired t-test; within right , M=-1.25%, SD=0.63%, $p = 0.005$, $CI = -1.9133 - (-0.5867)$ paired t-test) (Figure 3.9).

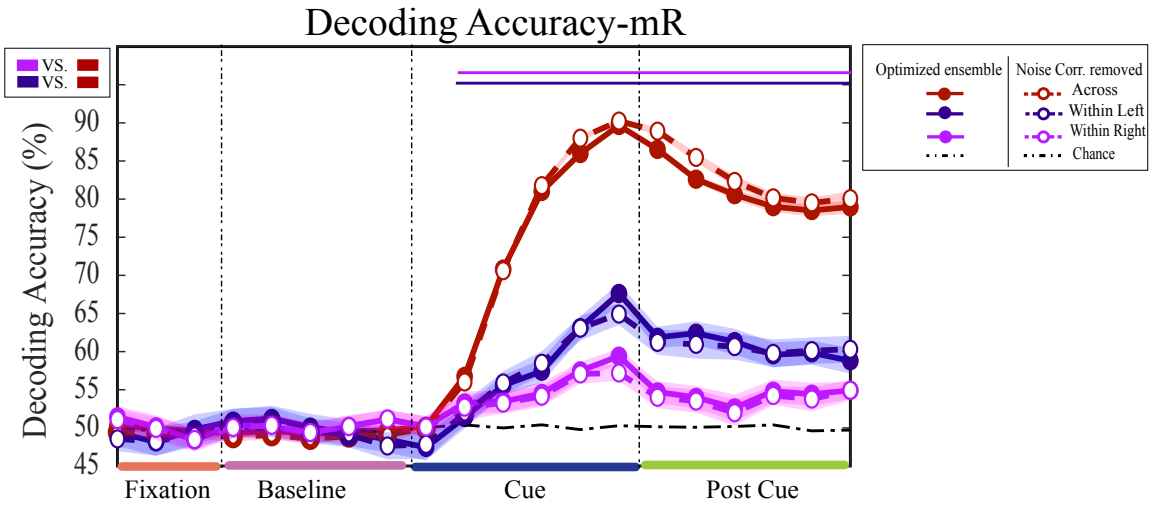

Figure 3.9: **Effects of Correlations on Information Coding**

Decoding accuracy using 400 ms window sliding with 100 ms window over time for optimized ensemble in the across (red line with close circles), within left (blue line with close circles) and within right (magenta line with close circles) conditions. Dashed lines with open circles represent decoding accuracy without noise. Black dashed dot line represents chance performance. Shading indicates SEM ($\pm$) for each time point. The straight lines at the top indicate statistically significant (Wilcoxon rank sum $p < 0.05$) differences between optimized ensemble performance in within left and within right conditions versus across condition.

Next, we asked how noise correlations change between conditions. To address this issue, we evaluated noise correlations between neurons in the recorded neuronal ensembles. Figure 3.10A illustrates variation of noise correlations between simultaneously recorded pairs of units versus time course of the experiment in the three conditions. Most correlations were positive, small, and almost constant across time in three conditions. We also quantified changes in noise correlations between attentional epochs by comparing the cumulative distribution function (CDF) of noise correlations in each epoch to others in three conditions (Figure 4.4).

Noise correlations between all possible pairs of units in the optimized ensemble were lower in across condition than within right and within left conditions (Figure 3.10A).

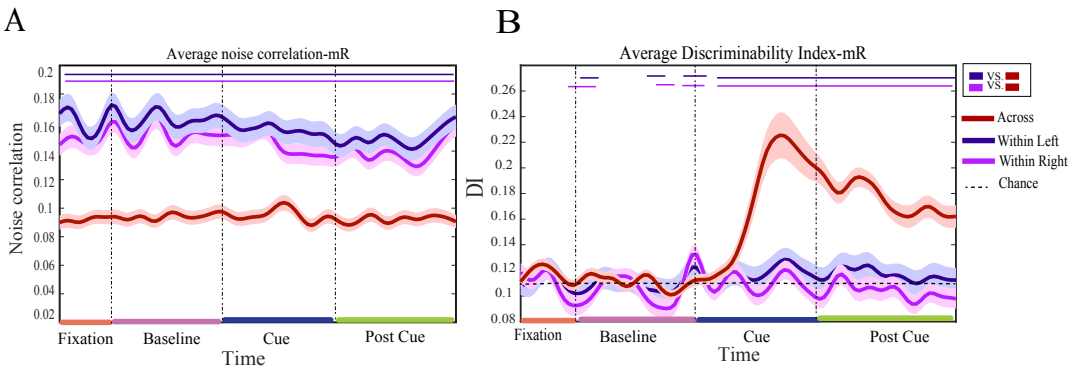

Figure 3.10: **Noise Correlation and Discriminability Index**

(A) Average noise correlation between all possible pairs in across (red line), within left (blue line) and within right (magenta line) conditions versus time. (B) Average discriminability index (DI) between all possible pairs of optimized ensemble versus time in across (red line), within left (blue line) and within right (magenta line) conditions. The dashed black line shows chance level. Shading indicates SEM ($\pm$) for each time point. The straight lines at the top indicate statistically significant (Permutation test $p < 0.05$) between across conditions versus within conditions.

3.5.4 Interaction Between Signal and Noise Correlations

Although noise correlations play different roles in decoding accuracy, it are not the only factor that affects information encoding [Arandia-Romero I. et al. 2016; Moreno-Bote et al. 2014]. We computed the discriminability index (DI, see methods) between each pair units comprising the optimized ensembles, which can be considered a measure that incorporates the population tuning (signal correlation) and the trial-by-trial variability (noise correlation) for each condition (Figure 3.10B). We found that DI was higher in the across than in the within conditions during the cue and post cue epochs of the task. However, considering that noise correlations were relatively stable in all task periods (Figure 3.10A), this effect is likely due to the emergence of selectivity (signal correlation) for the attended location during the cue and post cue task epochs.

Chapter 4

Disscusion

In this study, we investigated the behavioral and neural correlates of attentional filtering when two stimuli (target and distractor) are presented within the same hemifield as compared to when they are distributed across both hemifields. Consistent with previous psychophysical studies, we found that behavioral performance in a spatial attention task is significantly decreased when stimuli are presented in the same visual hemifield (Awh and Pashler, 2000; Delvenne and Holt, 2012). Moreover, we found that this behavioral effect is matched by corresponding neuronal correlates in the ability of LPFC ensembles to discriminate between attended targets and ignored distractors. LPFC is hypothesized to be critically involved in the allocation of visuospatial attention (Miller, 2000; Everling et al., 2002; Lennert et al., 2011; Tremblay et al., 2015). Here, we show that when two stimuli are presented in the same visual hemifield, neuronal discrimination of target from distractor is impaired. It is shown by 1) decreased proportion of location selective units 2) decreased sensitivity index (d') of single neurons, 3) decreased discriminability index (DI) for pairs of neurons, 4) reduced decoding performance from the neuronal ensemble. Importantly, we found that this difference in neural decoding performance seemed to be due to two variables: 1) a decrease in the selectivity of the individual units for the allocation of attention (signal correlation) and 2) an increase in trial-by-trial variability (noise correlations).

4.1 Filtering Distractors Within versus Across Hemifields

Psychophysical research suggests that attentional resources are independent, hemispheric-specific pools (Alvarez et al., 2012; Delvenne and Holt, 2012; Walter et al., 2015). Al-

though this is well interested within the behavioral literature and theoretical models of attention, the physiological meaning of this statement is unclear. Our data shows that attentional filtering by single neurons and neuronal ensembles in LPFC is diminished when monkeys allocated visuospatial attention to one of two stimuli when they were presented in the same hemifield relative to when they were presented in different hemifields. A study by Buschman and colleagues (2011) has demonstrated that neuronal information in LIP and LPFC about an object's identity was reduced when another object was in the same as compared to the opposite visual field. To place these findings within the known anatomy and physiology of the prefrontal cortex, it is possible that two stimuli distributed across and within the same hemifield activate distinct cortical columns of neurons tuned for the stimuli location. (Goldman-Rakic et al., 1982; Hirata et al., 2008; Matsushima et al., 2014). The competition for the focus of attention between groups of neurons/columns may be better resolved when it takes place between columns where neurons are tuned for stimuli in different visual hemifields than when they are tuned for stimuli within the same visual hemifield, even when the physical distance between stimuli in retinotopic coordinates is similar. It is also possible that stimuli in both hemifields are processed relatively independently whereas stimuli within the same visual hemifield activating shared connections between neurons differentially tuned decreasing the effectivity of the competition, which likely happens through inhibitory connections (Matsushima et al., 2014; Reynolds et al. 1999).

One possible criticism to our study is that the distance between the centers of the two RDPs was not the same for the tasks (16° in the across and 11.33° in the within task). We chose to keep the patterns at the center of the screen at the level of the fixation point in the across condition to compare the data with a previous experiment using the same configuration. This made us to position the patterns slightly closer in the within hemifields configuration to keep eccentricity constant between the two configurations. One may argue that the closer stimuli were much harder to attend to. This is possible, however, in our experience the dis-

tance between stimuli was still large enough to not significantly increase task difficulty. Humans are reasonably able to identify and discriminate between stimuli separate by 5° at 10° eccentricity (Whitney et al., 2011; Rovamo et al. 1982). Thus, crowding effects in the periphery were unlikely to account for our results .

4.2 Decoding from Neuronal Ensembles

Using our ensemble building approach, we were able to decode the location of the target stimulus reliably above chance, even in instances when the entire population yielded only chance performance and only very few units were selective for the target location. It has been shown that stimulus information can be distributed across a neuronal population without being strongly present in single units (Rigotti et al., 2013). In our approach, we were unable to search the entire space of possible n-sized ensembles due to time and computing power restrictions. Repeating the analysis using all possible neuron combinations instead of keeping the best duo, trio, etc, would avoid potential overfitting to noisy signals. However, this approach is unrealistic in a reasonable amount of time with the computational power we have available. Thus, although searching the entire space of neuronal ensembles may have at least theoretically led to a different estimation we believe that the main result is unlikely to change.

Simultaneously active neurons show complex population mechanisms, which are difficult to measure (Arandia-Romero et al., 2016). We found that by measuring discriminability index (DI) (Moore et al., 1970; Shadlen and Newsome, 1998), and population activity (see methods for details) can assess neuronal interactions and thus gain insight into how the brain encodes information. Several studies have reported mixed results about the contribution of noise correlations to stimulus encoding (Nirenberg et al., 2003; Averbeck et al., 2006; Ruff et al., 2014; Tremblay et al., 2015). In our data, removing noise correlations from neuronal ensembles also yielded mixed results. In the data recorded, for the across condition task, removing noise correlations modestly improved decoding accuracy

suggesting that interactions between pairs of neurons were detrimental to the amount of information regarding spatial attention a neuronal ensemble contained. In contrast, the same procedure for the within condition task caused a slight decrease in decoding accuracy. However, it is important to note that the overall impact on information coding in our data was relatively small. These results suggest that in our data noise correlation did not greatly influenced information coding.

On the other hand, we estimated DI (see methods) which can be considered a measure of population tuning (signal correlation) and trial-by-trial variability (noise correlation) for each condition. Interestingly, we found that DI robustly predicted the decoding accuracy and identifies the features of neuronal population activity that most affect information encoding. This suggest that signal correlation had the strongest impact in the encoded information by neuronal ensembles.

4.3 Stationarity of Recordings

One possible criticism to our study is that we did not record from the same neurons in the within and across conditions. This was due to the complexity of the task and analyses that required a large number of trials for each condition. This could in principle introduce non-stationary confounds to the recorded data that covey with the decreased performance (e.g., decreased signal to noise ratio of the array). However, our electrodes penetrated the cortex orthogonal to the surface and likely sampled neurons within the same cortical columns. Moreover, previous studies have shown that signals remain relatively stable across recording days in terms of their selectivity for the allocation of attention using similar arrays (e.g., Tremblay et al, 2015). Furthermore, the percentage of task-related units and the overall average firing rate of neurons recorded under both conditions were similar, suggesting that the observed phenomena reflect a change in the neural representation of attended locations, rather than any non-stationarities in our recordings.

4.4 General Conclusion

Our study indicated that behavioral anisotropy observed during tasks that required attending to target and distractors in different versus same hemifields is correlated with neural performance in LPFC. They further suggest that anisotropies in the representation of space by individual neurons and neuronal ensembles in the LPFC determine the efficiency of attentional filtering performance in primates. A modest explanation for these behavioral anisotropy from the view of neuronal computation is that having visual input on both hemifields would cause neuronal activity in independently processing pools and spared in distinct cortical columns. Independent processing decreases noise correlation and increases population tuning. This cause high amount of information carries by neural population. In contrast, when only one processing pool receives visual input, increased noise correlation reflects positive feedback and population tuning decreases. Thus information encoded by neural ensemble decreases.

Taken together, these results will provide new insight into the neural mechanisms underlying visual attention within the LPFC and stress the importance of examining population activity in cognitive neurophysiology. Further implications of this project should be considered in the context of clinical populations living with attention disorders.

References

Alvarez G.A., Gill J., Cavanagh P. (2012) Anatomical constraints on attention: Hemifield independence is a signature of multifocal spatial selection, Journal of Vision 12:1-20.

Arandia-Romero I., Tanabe S., Drugowitsch J., Kohn A., Moreno-Bote R. (2016) Multiplicative and Additive Modulation of Neuronal Tuning with Population Activity Affects Encoded Information, Neuron 89:1305-1316.

Asaad W. F., Rainer G., Miller E. K. (1998) Neural Activity in the Primate Prefrontal Cortex during Associative Learning, Neuron, 21, 1399-1407.

Averbeck B.B., Latham P.E., Pouget A. (2006) Neural correlations population coding and computation, Nature Reviews Neuroscience, 7:358-366.

Awh E., Pashler H. (2000) Evidence for split attentional foci, Journal of Experimental Psychology: Human Perception and Performance, 26(2), 834-846.

Backen T., Treue S., Martinez-Trujillo J.C. (2018) Encoding of spatial attention by primate prefrontal cortex neuronal ensembles, eNeuro, 0372-16.2017.

Bugbee NM, Goldman-Rakic PS. (1983) Columnar organization of corticocortical projections in squirrel and rhesus monkeys: similarity of column width in species differing in cortical volume, The Journal of Comparative Neurology, 220(3):355-64.

Buschman T.J., Kastner S. (2015) From behavior to neural dynamic: an integrated theory of attention, Neuron, 88 (1): 127-44.

Buschman T.J., Siegel M., Roy J.E., Miller E.K. (2011) Neural substrates of cognitive capacity limitations, PNAS, 108:11252-11255.

Buschman T. J., Miller E. K. (2009) Serial covert shifts of attention during visual search are reflected by the frontal eye fields and correlated with population oscillations, Neuron, 63(3): 386-96.

Buschman T. J., Miller E. K. (2007) Top-Down Versus Bottom-Up Control of Attention in the Prefrontal and Posterior Parietal Cortices, Science 315, 5820.

Carrasco M., (2011) Visual attention: the past 25 years, Vision Research, 51(13).

Carrasco M., Giordano A.M., McElree B. (2006) Attention speeds processing across eccentricity: Feature and conjunction searches, Vision Research 46:2028-2040.

Castiello U., Umilta C. (1990) Size of the attentional focus and efficiency of processing, Acta Psychologica 73, 195-209.

Cohen M.R., Kohn A. (2011) Measuring and interpreting neuronal correlations, Nature Neuroscience 14:811-819.

Delvenne J.-F., Holt J.L. (2012) Splitting attention across the two visual fields in visual short-term memory, Cognition 122:258-263.

Desimone R., Duncan J. (1995) Neural mechanisms of selective visual attention, Annual Reviw Neuroscience, 18, 193-222.

Everling S., Tinsley C.J., Gaffan D., Duncan J. (2002) Filtering of neural signals by focused attention in the monkey prefrontal cortex, Nature Neuroscience 5:671-676.

Fan R.-E., Chang K.-W., Hsieh C.-J., Wang X.-R., Lin C.-J. (2008) LIBLINEAR: A library for large linear classification, The Journal of Machine Learning Research, 9:1871-1874.

Fecteau J. H., Munoz D. P. (2006) Salience, relevance, and firing: a priority map for target selection, TRENDS in cognitive science, 10, 8.

Fuller S., Rodriguez R.Z., Carrasco M. (2008) Apparent contrast differs across the vertical meridian: Visual and attentional factors. J Vis 8:1-16.

Genovesio A., Brasted P. J., Wise S. P. (2006) Representation of Future and Previous Spatial Goals by Separate Neural Populations in Prefrontal Cortex, The Journal of Neuroscience, 26(27): 7305-7316.

Gregoriou G. G., Rossi A. F., Ungerleider L. G., Desimone R. (2014) Lesions of prefrontal cortex reduce attentional modulation of neuronal responses and synchrony in V4, Nature Neuroscience, 17(7): 1003-1011.

Green J. D. (1958) A simple microelectrode for recording from the central nervous system, Nature 182,962.

Goldman-Rakic P. (1987) Development of cortical circuitry and cognitive function, Child Dey, 58(3) 601-22.

Goldman-Rakic P., Schwartz M. (1982) Interdigitation of contralateral and ipsilateral columnar projections to frontal association cortex in primates, science 216:755-757.

Hanes D., Schall J. (1996) Neural Control of Voluntary Movement Initiation, Science, Vol 274, Issue 528.

Hubel DH. (1957) Tungsten microelectrode for recording from single units, Science, 125: 549-50.

Hirata Y., Sawaguchi T. (2008) Functional columns in the primate prefrontal cortex revealed by optical imaging in vitro, Neuroscience Research 61:1-10.

James W. (1890) The principles of psychology, Henry Holt and company.

Kelly R., Smith M., Samonds J., Kohn A., Bonds A., Movshon J and Lee T (2007) Comparison of Recordings from Microelectrode Arrays and Single Electrodes in the Visual Cortex, Journal of Neuroscience, 27 (2) 261-264.

Laberage D., Brown V. (1986) Variation in size of the visual field in which targets are presented: An attentional range effect, Perception & Psychophysics, 40(3), 188-200.

Laughlin SB, Sejnowski TJ. (2003) Communication in neuronal networks, Science, 301.

Lebedev M.A., Messinger A., Kralik J.D., Wise S.P. (2004) Representation of attended versus remembered locations in prefrontal cortex, PLoS Biol. 2, e365.

Lennert T., Martinez-Trujillo J. (2011) Strength of response suppression to distracter stimuli determines attentional-filtering performance in primate prefrontal neurons, Neuron 70:141-152.

Lennert T., Martinez-Trujillo J.C. (2013) Prefrontal neurons of opposite spatial preference display distinct target selection dynamics, Journal Neuroscience 33:9520-9529.

Leavitt M. L., Pieperc F., Sachsd A. J., and Martinez-Trujillo J. C. (2017) Correlated variability modifies working memory fidelity in primate prefrontal neuronal ensembles, PNAS, E2494–E2503.

Levy WB., Baxter RA. (1996) Energy efficient neural codes, neural computation 8(3): 531-43.

Ipata A. E., Gee A. L., Bisley J. W., Goldberg M. E. (2009) Neurons in the lateral intraparietal area create a priority map by the combination of disparate signals, Experimental Brain Research, 192(3): 479-488.

MacLean K., Aichele S., Bridwell D., Mangun G., Wojciulik E., Saron C. (2009) Interactions between Endogenous and Exogenous Attention during Vigilance, Attention Perception Psychophysics, 71(5): 1042–1058.

Martinez-Trujillo J., Treue S. (2004) Feature-based attention increases the selectivity of population responses in primate visual cortex, Current Biology, 14 (9): 744-51.

Matsushima A., Tanaka M. (2014) Different neuronal computations of spatial working memory for multiple locations within versus across visual hemifields, Journal Neuroscience 34:5621-5626.

Mayo P., Cohen M., Maunsell J. (2015) A Refined Neuronal Population Measure of Visual Attention, PLOS ONE, 0136570.

Miller E.K. (2000) The prefontral cortex and cognitive control, Nature Reviw Neuroscience 1:59-65.

Miller E.K., Erickson CA., Desimone R. (1996) Neural mechanisms of visual working memory in prefrontal cortex of the macaque, Journal Neuroscience, 16(16): 5154-67.

Moore G.P., Segundo J.P., Perkel D.H., Levitan H. (1970) Statistical Signs of Synaptic Interaction in Neurons, Biophys Journal 10:876-900.

Moran J., Desimone R. (1985) Selective attention gates visual processing in the Extrastriate cortex, Science, 229.

Moreno-Bote R., Beck J., Kanitscheider I., Pitkow X., Latham P. and Pouget A. (2014) 'Information-limiting correlations ', nature neuroscience, volue 17, number 10.

Murray J. D., Bernacchia A. , Roy N. A., Constantinidis C., Romo R., Wang X (2017) 'Stable population coding for working memory coexists with heterogeneous neural dynamics in prefrontal cortex', PNAS , vol. 114 , no. 2, 394–399.

Nirenberg S., Latham P.E. (2003) Decoding neuronal spike trains: How important are correlations? Proc Natl Acad Sci 100:7348-7353.

Paulun L., Wendt A., Kasabov N. (2018) A Retinotopic Spiking Neural Network System for Accurate Recognition of Moving Objects Using NeuCube and Dynamic Vision Sensors, Frontiers in Computational Neuroscience, Volume 12, Article 42

Petrides M., Tomaiuolobc F., H.Yeteriandef E., N.Pandyaefg D. (2012) The prefrontal cortex: Comparative architectonic organization in the human and the macaque monkey brains, Cortex, Volume 48, Issue 1, Pages 46-57.

Rigotti M., Barak O., Warden M.R., Wang X.-J., Daw N.D., Miller E.K., Fusi S. (2013) The importance of mixed selectivity in complex cognitive tasks, Nature 497:585-590.

Rossi A. F., Bichot N. P., Desimone R. , Ungerleide L. G. (2007) Top–Down Attentional Deficits in Macaques with Lesions of Lateral Prefrontal Cortex, The Journal of Neuroscience, 27(42): 11306-11314.

Rovamo J., Virsu V., Laurinen P., Hyvärinen L. (1982) Resolution of gratings oriented along and across meridians in peripheral vision, Investigative Ophthalmology & Visual Science 23:666-670.

Ruff D.A., Cohen M.R. (2014) Attention can either increase or decrease spike count correlations in visual cortex, Nature Neuroscience 17:1591-1597.

Schall J. D. (2002) The neural selection and control of saccades by the frontal eye field, Philosophical Transactions of the Royal Society of London, Series B, Biological Science, 357, 1073–1082.

Shadlen M.N., Newsome W.T. (1998) The variable discharge of cortical neurons: implications for connectivity, computation, and information coding, Journal Neuroscience 18:3870-3896.

Spitzer H., Desimone R., Moran J (1998) Increased attention enhances both behavioral and neuronal performance, Science, Vol 240, Issue 4850.

Steveninck R. R. de Ruyter, Laughlin S. B. (1996) The rate of information transfer at graded-potential synapses, NATYRE 379.

Störmer V.S., Alvarez G.A., Cavanagh P. (2014) Within-hemifield competition in early visual areas limits the ability to track multiple objects with attention, Journal Neuroscience 34:11526-11533.

Szczepanski S. M., Knight R. T. (2014) Insights into Human Behavior from Lesions to the Prefrontal Cortex, Neuron, 83(5): 1002-1018.

Thompson K.G., Bichot N.P. (2005) A visual salience map in the primate frontal eye field, Progress in Brain Research, 147, 249-262.

Tremblay S., Pieper F., Sachs A., Martinez-Trujillo J.C. (2015) Attentional filtering of visual information by neuronal ensembles in the primate lateral prefrontal cortex, Neuron 85:202-215.

Treue S., Martinez Trujillo J (1999) Feature-based attention influences motion processing gain in macaque visual cortex, NATURE, VOL 399.

Vandenberghe R., Duncan J., Arnell K.M., Bishop S.J., Herrod N.J., Owen A.M., Minhas P.S., Dupont P., Pickard J.D., Orban G.A. (2000) Maintaining and Shifting Attention within Left or Right Hemifield, Cerebral Cortex 10:706-713.

Yantis S. (2008) The neural basis of selective attention, Current Directions in Psychological Science, 17(2): 86-90.

Walter S., Keitel C., Müller M.M. (2015) Sustained Splits of Attention within versus across Visual Hemifields Produce Distinct Spatial Gain Profiles, Journal Cognitive Neuroscience 28:111-124.

White I.M., Wise S.P (1999) Rule-dependent neuronal activity in the prefrontal cortex, Experimental Brain Research, 126 (3): 315-35.

Whitney D., Levi D.M. (2011) Visual crowding: a fundamental limit on conscious perception and object recognition, Trends in cognitive sciences 15:160-168.

Supplemental Figures

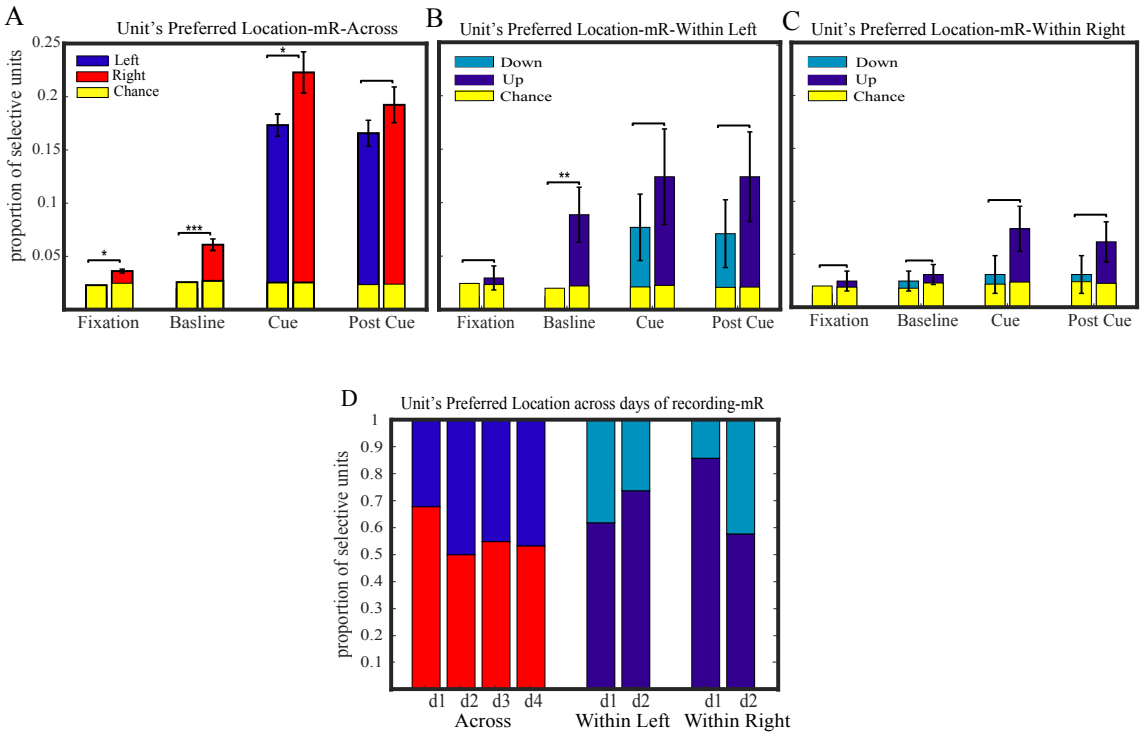

Figure 4.1: **Single Unit Selectivity**

(A) Proportion of unit's preferred location in across (one-way ANOVA with factor target location, $p < 0.05$), (B) within left and (C) within right conditions for four different epochs. Red bars represent unit's selective for target in right side of fixation point (contralateral of recording), blue bars represent unit's selective for target in left side of fixation point (ipsilateral of recording), turquois bars represent unit's selective for target under fixation point, dark blue bars represent unit's selective for target above fixation point and yellow bars show chance level. Error bars represents SEM ($\pm$) over recording sessions. Asterisks mark significant differences in mean proportion (χ^2-test; * $p < 0.05$, ** $p < 0.01$, *** $p < 0.001$). (D) Proportion of location selective units in each recording sessions to see whether the distributions of location selective units were approximately stable over recording sessions.

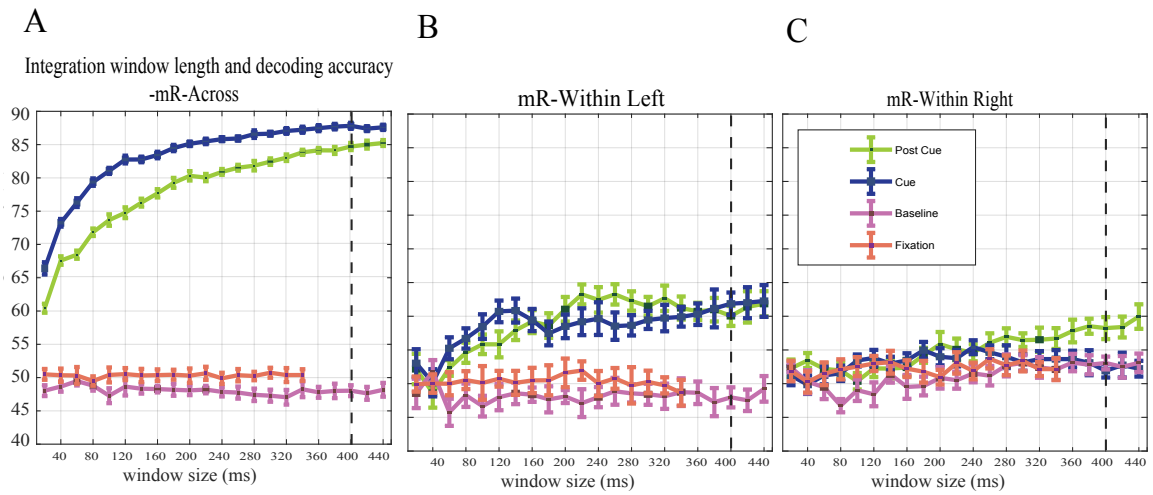

Figure 4.2: **Decoding Accuracy vs. Integration Window**

Integration windows of different lengths are tested during the fixation (orange lines), baseline (magenta lines), cue (dark blue lines) and postcue (light green lines) periods. Firing rates are computed over such windows for all unit part of an ensemble and entered into the logistic regression (LR) classifier for training and testing. The fixation and baseline windows are started from t=1ms and t=400ms after fixation point appears on the screen respectively. Cue epoch is cantered on the epoch 500 ms after the cue onset. The post cue window is started 50 ms after cue offset. The black dotted line represents the chosen window size. (A-C) across, within left and within right conditions.

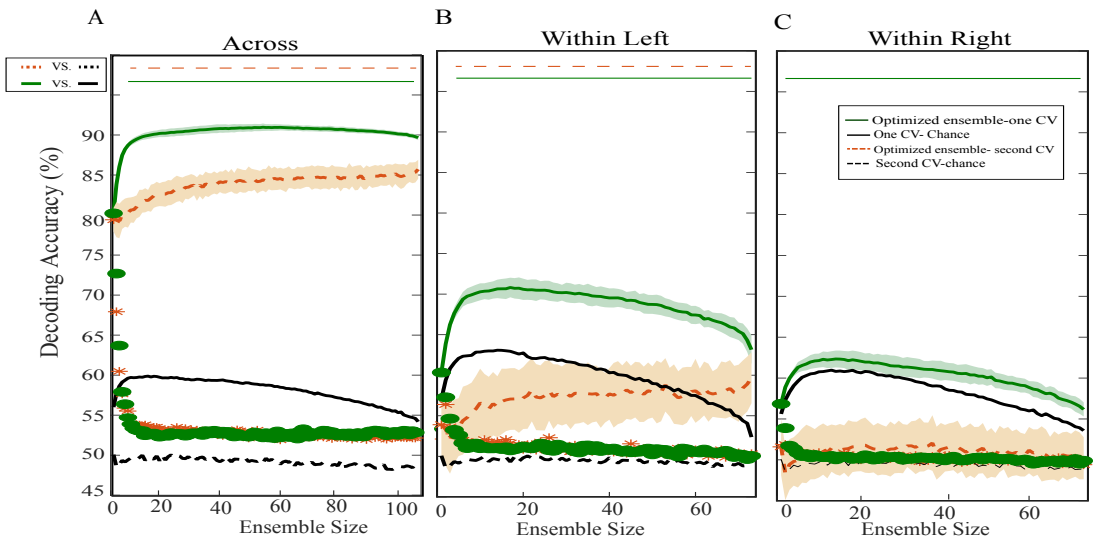

Figure 4.3: **Ensemble Decoding of Target Location**

Decoding accuracy using 400 ms window centered 500 ms after cue onset from increasingly larger ensembles according to optimized method in the (A) across, (B) within left and (C) within right conditions. Dashed orange lines represent decoding accuracy by using second cross validation. Shading indicates SEM ($\pm$) for each ensemble size. Dots show accuracy of single units that add in each optimized ensemble size. Stars represent mean accuracy of single units after second cross validation. The solid black line symbolizes chance performance for optimized ensemble and dashed black line shows chance performance after second cross validation.The straight lines at the top indicate statistically significant between ensembles performance vs. their chance performance (Wilcoxon rank sum $p < 0.05$).

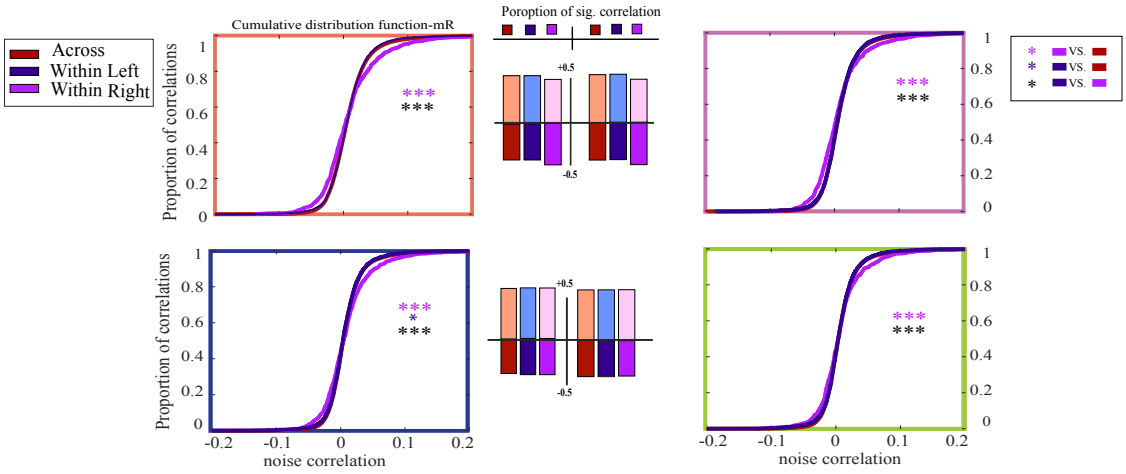

		Baseline-Cue	Baseline-Postcue	Cue-Postcue
R	Across	***	***	***
	Within Left	**	***	*
	Within Right	**	**	*

Figure 4.4: **Distribution of Mean noise Correlation Across Task Epochs**

(A) Cumulative distribution function of noise correlation in each time epoch fixation (orange), baseline (magenta), cue (dark blue) and post cue (light green) for across (red line), within left (blue line) and within right (magenta line) conditions. Stars show statistically significant (Kolmogorov test , *: $0.01 < p < 0.05$, **: $10^{-4} < p < 10^{-2}$ and *** $p < 10^{-4}$) (B) Comparison between cumulative distribution function of noise correlation in each condition between three time epochs. Stars show statistically significant (Kolmogorov test, *: $0.01 < p < 0.05$, **:$10^{-4} < p < 10^{-2}$ and *** $p < 10^{-4}$).

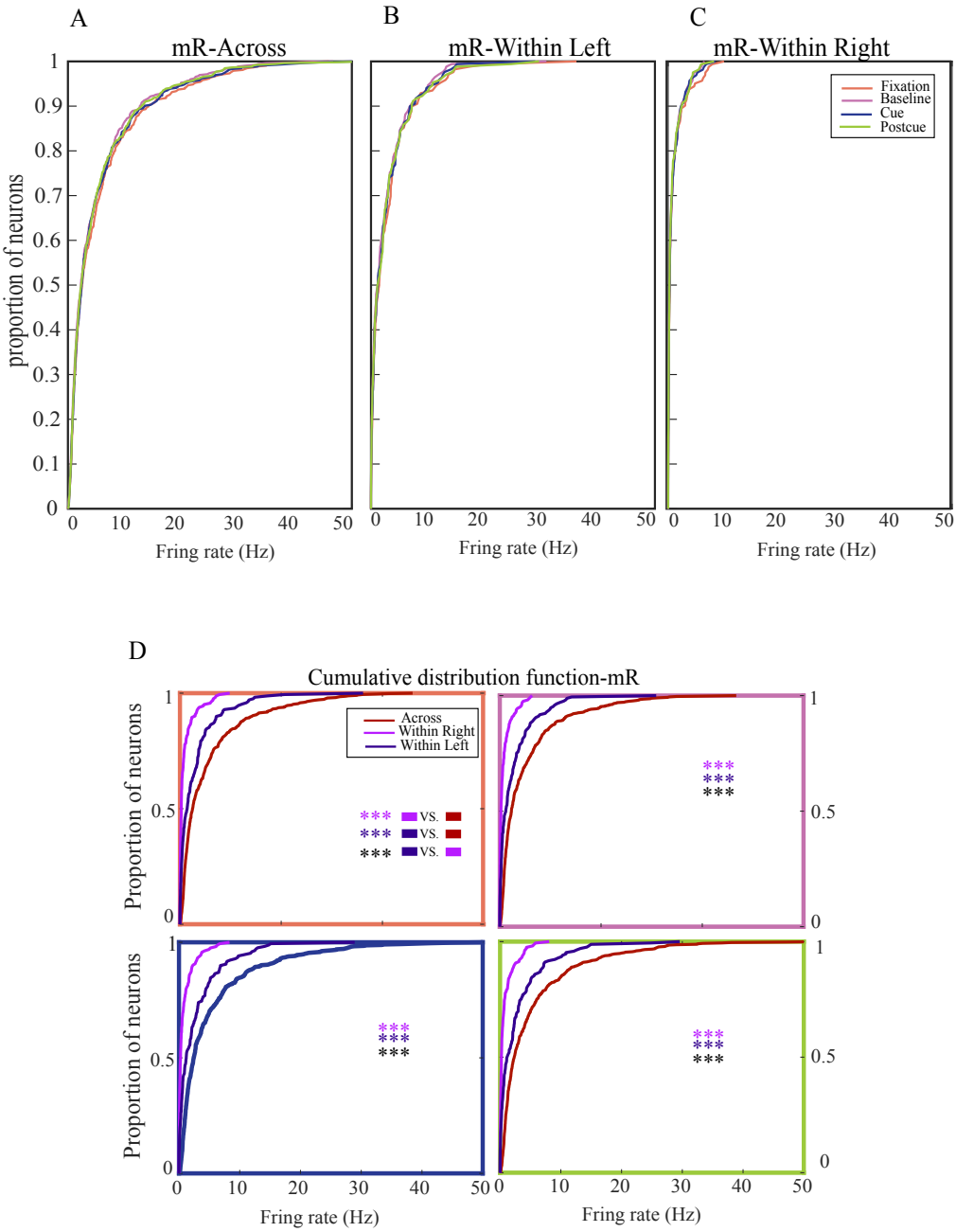

Figure 4.5: **Distribution of Mean Firing Rates Across Task Epochs**

Cumulative distribution function (CDF) of mean firing rate across neurons in four task epochs in (A) across, (B) within left and (C) within right conditions. Orange, magenta, dark blue and light green lines show fixation, baseline, cue and postcue epochs respectively. Interestingly, when compared across task epochs in each condition the overall distribution of firing rates does not change significantly ($p \sim 0.7$, two-sample Kolmogorov-Smirnoff test). (D) Cumulative distribution function (CDF) of mean firing rate across neurons in four task epochs in across (red line), within left (dark blue line) and within right (magenta line) conditions. Orange, magenta, dark blue and light green boxes show fixation, baseline, cue and postcue epochs respectively. CDF of firing rates significantly change between conditions especially across versus within conditions ($p < 10^{-4}$, two-sample Kolmogorov-Smirnoff test).

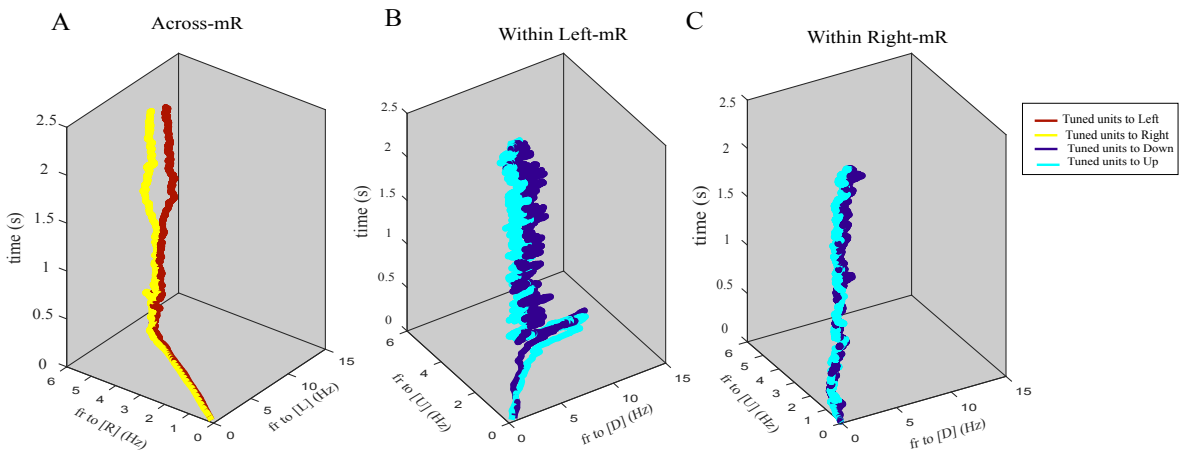

Figure 4.6: **Neural Trajectory**

Population firing rate trajectories over time course of experiment in target location selective unit's space. Here x and y-axes show response to right/up and left/down respectively. The z-axis is an orthogonal axis in this space that captures time-related activity. Each trace corresponds to mean average response of one type of location selective neurons. Left and right location selective neurons in across condition correspond to red and yellow trace, up and down location selective neurons in within conditions correspond to cyan and dark blue respectively. The shading of the traces indicates SEM.

Vita

Maryam Nouri Kadijani

Education

- B.S., Solid state Physics, Kharazmi University, Tehran, Iran, 2003-2007

- M.Sc., Plasma Physics, Amirkabir University of Technology, Tehran, Iran, 2007-2010

- M.Sc, Neuroscience, University of Western Ontario, London, Ontario, Canada, 2017-2019

Supervisors: Dr. Julio Martinez-Trujillo & Dr. Jörn Diedrichsen

Awards and Honors

- 2017, International Graduate Student Scholarship (IGSS) in Cognitive Neuroscience, University of Western Onario, London, Ontario, Canada, $ 15000 per year (up to 2 years).

- 2010, Ranked 1st among physics Graduate students in Dept. of Energy Engineering and Physics, Amirkabir University of Technology, Tehran, Iran.

- 2007, Ranked 1st among physics Undergraduate students in Dept. of Physics, Kharazmi University of Technology, Tehran, Iran.

Published or Working Papers

- Neural correlates of enhanced attentional filtering of distractors across vs. within visual hemifields in the lateral prefrontal cortex, Maryam Nouri Kadijani, Theda Backen, Stefan Treue, Julio C. Martinez-Trujillo, Jörn Diedrichsen (working paper)

Workshop

- Summer school in computational neuroscience, University of Ottawa, Ottawa, Ontario, Canada, (2018).